

Extended mixed model for association mapping with growth response curve

Recall that the salt stress induced growth response is measured as the square root transformed ratio of the projected shoot area (PSA) of plants under salt stress over that of plants under normal growth situations. For each single SNP, the mean response curve of a specific genotype k (1 or 2 for the two alleles) is modeled as a decreasing logistic function:

$$f_k(t) = \gamma + \frac{(1 + \beta_k)(1 - \gamma_k)}{1 + \beta_k e^{\alpha_k t}}$$

where t is the time, α , β and γ are regression coefficients. Note that this function is nonincreasing, it is 1 at time zero, and it will flatten out as time becomes really long. These are reasonable assumptions for the salt response curve as all plants are under normal growing conditions at time zero, the salt stress has a detrimental effect on the growth on average, and growth will slow for all plants near the end of the growing period.

The growth response for line i with genotype k at time t (day 0 to day 17) is then designated as

$$y_{it} = f_k(t) + \varepsilon_{it}.$$

Here ε_{it} is the error term that incorporates the correlation structure both through time and between lines (kinship). Let $\varepsilon_i = (\varepsilon_{i0}, \dots, \varepsilon_{i17})$ be the vector of responses for line i , then

$$\text{Cor}(\varepsilon_i) = \begin{bmatrix} 1 & \rho & \dots & \rho^{17} \\ \rho & 1 & \dots & \rho^{16} \\ \dots & \dots & \dots & \dots \\ \rho^{16} & \rho^{15} & \dots & 1 \end{bmatrix}.$$

Thus, for a single line, the model reduces to a nonlinear mixed model with a first order auto regressive covariance structure. On the other hand, let $\varepsilon_t = (\varepsilon_{1t}, \dots, \varepsilon_{360t})$ be the vector of the response of all lines at time t , we have

$$\text{Cov}(\varepsilon_t) = \sigma_g^2 K + \sigma_e^2 I$$

where K is the kinship matrix between lines, I is a 360 by 360 identity matrix, σ_g^2 is the genotype variance component, and σ_e^2 is the error variance component. Thus, considering a single time point, we have exactly the same model used by other researchers in plant association mapping studies.

To consider correlation both across time and across lines, let

$$\varepsilon = \text{vec}([\varepsilon_{it}])$$

where the vec operator stacks columns of a matrix into a single vector. We assume that the covariance matrix

$$\Sigma = \text{Cov}(\varepsilon) = \text{Cov}(\varepsilon_t) \otimes \text{Cor}(\varepsilon_i)$$

with \otimes being the kronecker product. Further, we assume that the response y_{it} has a normal distribution with the mean defined by the function $f_k(t)$ and the variance matrix given by Σ . As a result, the likelihood ratio test on whether $f_k(t)$ is the same for $k=1,2$ can be carried out as usual with the likelihood defined by the normal distribution.

Statistical analysis of phenotypic data

Data derived from fluorescence and RGB/VIS images were combined across experiments, and a linear model was fit to calculate the adjusted means for each individual accession using the `lsmeans` function in the LSMeans package in R (R Core Team, 2014; Lenth and Hervé, 2015). The linear model included experiment and treatment as fixed effects, and accession as a random effect. The adjusted means were used for phenotypic analysis and GWA of fluorescence traits, as well as phenotypic analysis of PSA.

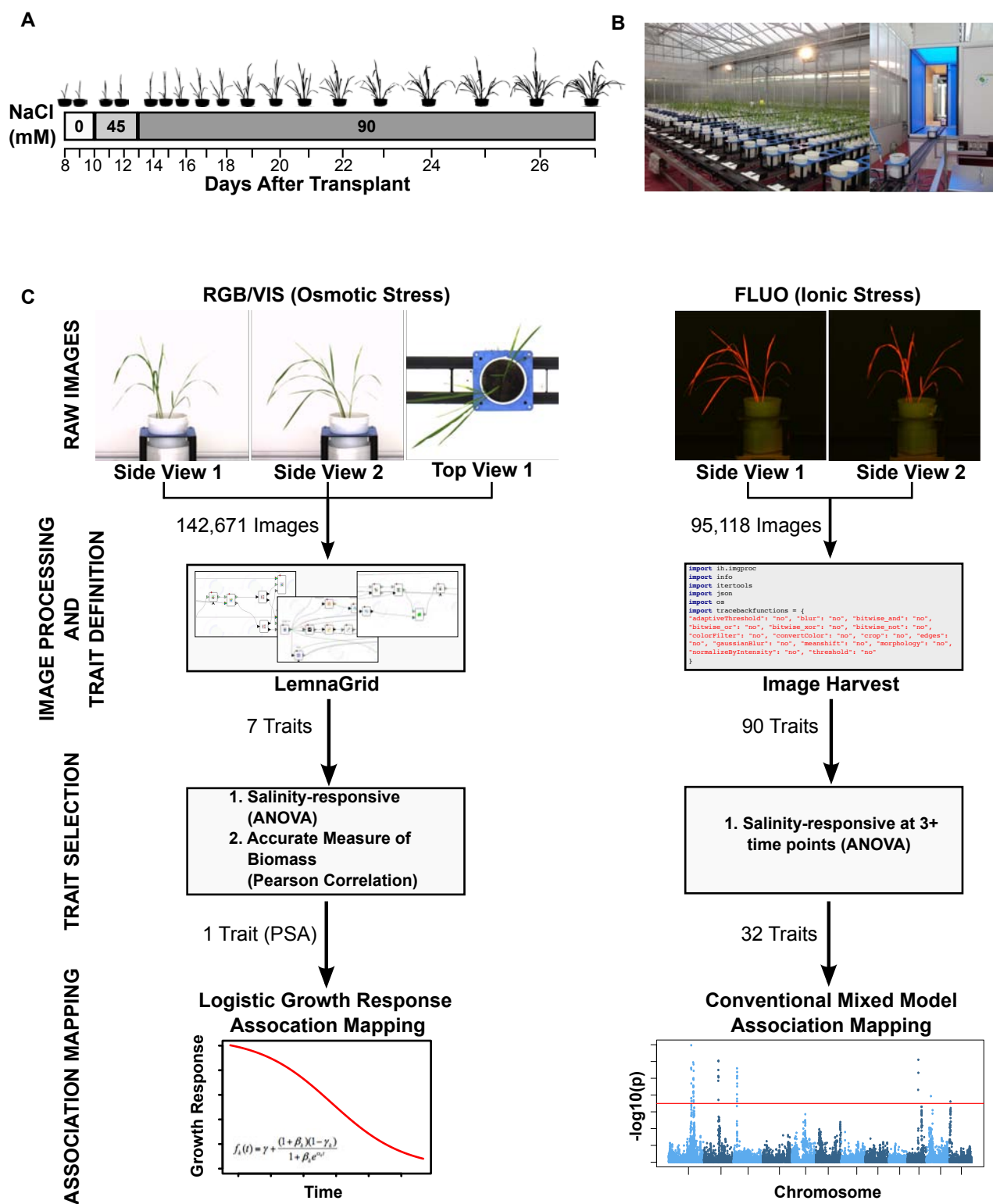


Fig S1: Schematic illustrating the experimental design and pipeline for the analysis of high-throughput phenotyping data. (A) Implementation of 90 mM NaCl. (B) High-throughput phenotyping of rice plants at the early-tillering stage using the LemnaTec system at the Plant Accelerator. (C) Workflow for image acquisition, processing and analysis (see Materials and Methods for a complete description).

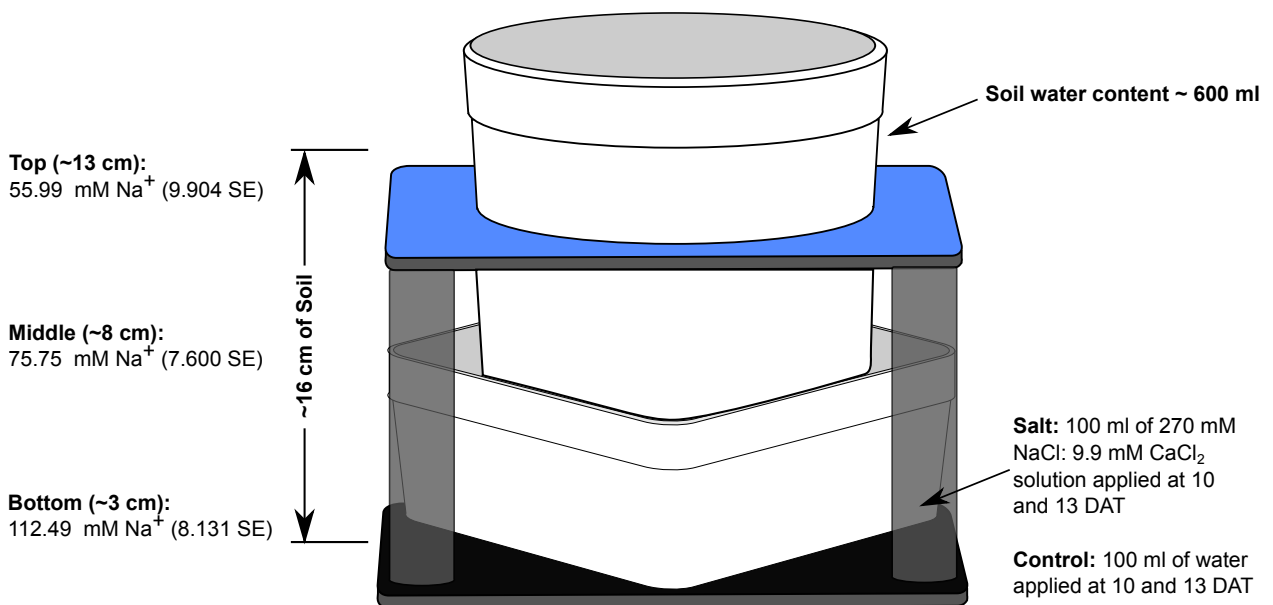


Figure S2. Schematic illustrating NaCl application. The salt treatment was applied by adding 100 ml of NaCl solution (270 mM NaCl: 9.9 mM CaCl₂) the square dish beneath the pot. The treatment was applied in two steps of 45 mM to reach a final concentration of 90 mM, at 10 and 13 DAT. Soil sodium concentration throughout the soil profile is listed on the left. DAT: Days after transplant.

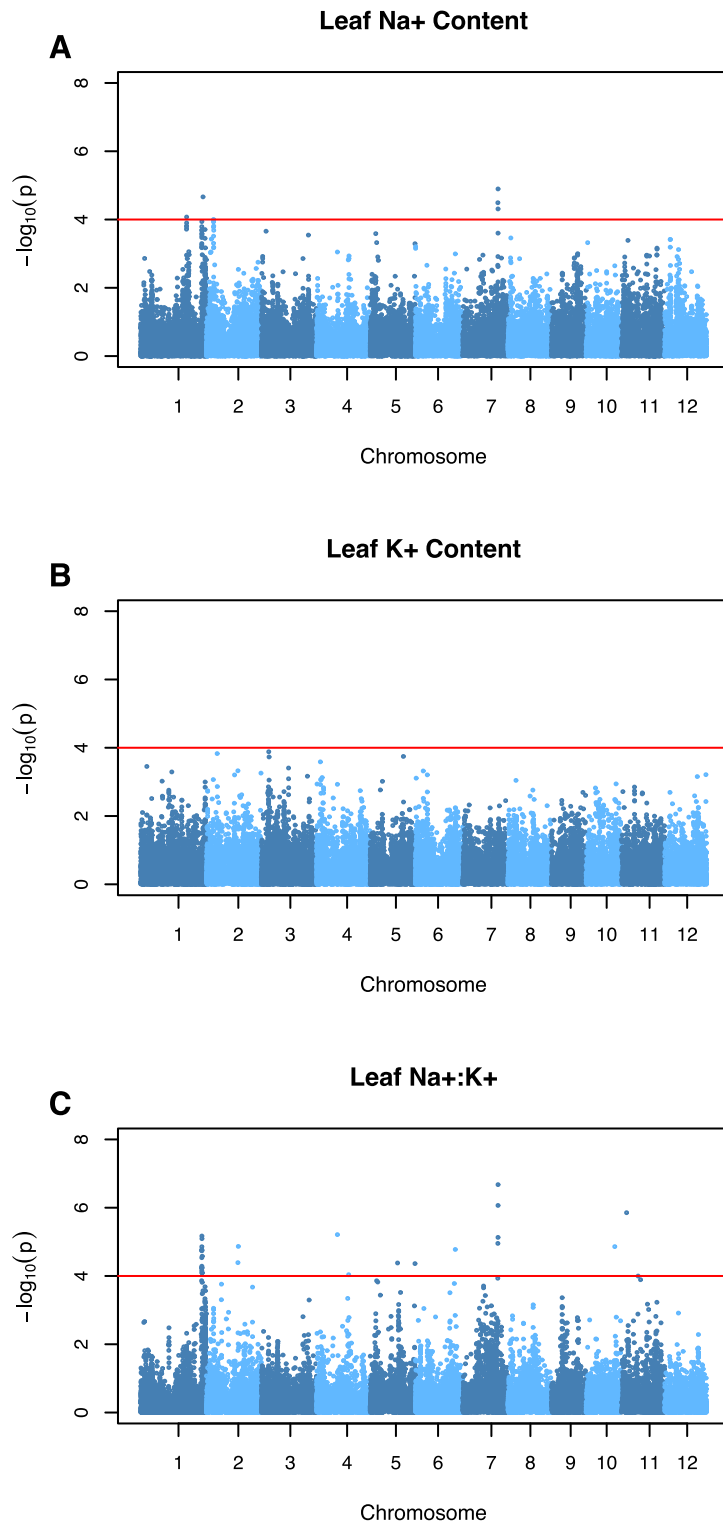


Fig S3: GWA analysis of leaf Na⁺ (A), K⁺ (B) and Na⁺:K⁺ content (C). The third leaf was collected at day 15 after 90 mM NaCl. The red horizontal line indicates statistical significance ($p < 10^{-4}$).

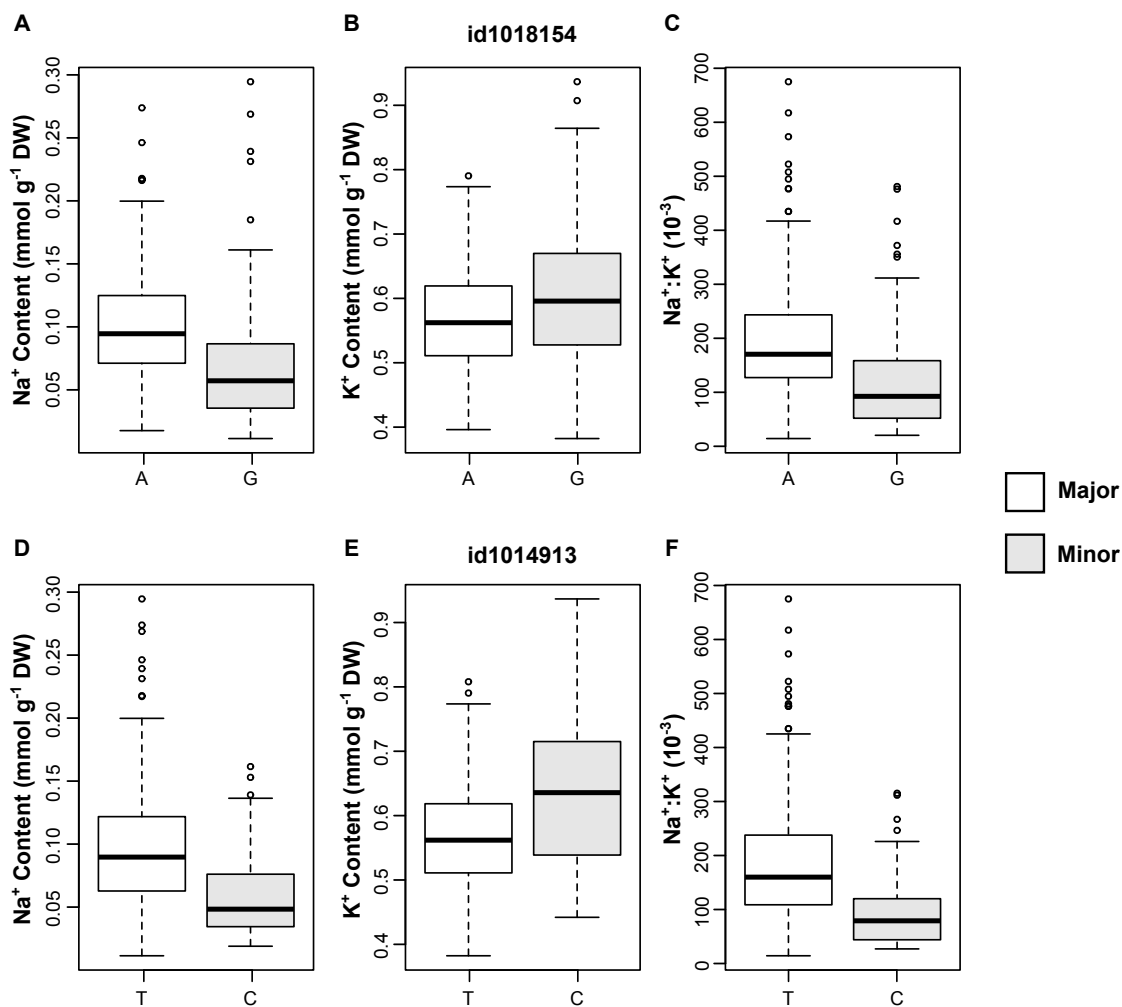
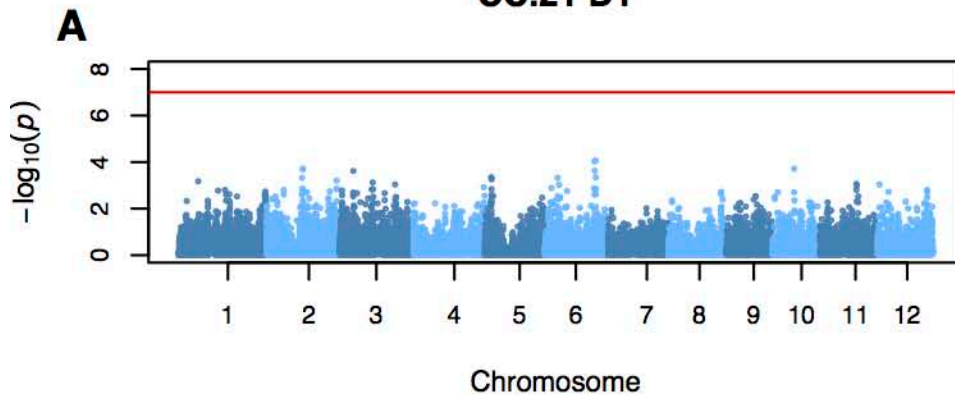


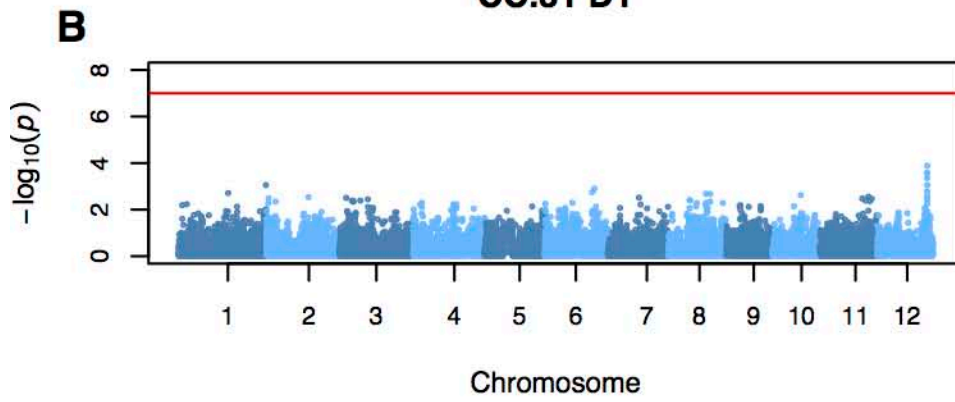
Fig S4: Distribution of leaf ion content observed between allelic groups at id1018154 (A-C) and id1014913 (D-F). (A) The minor allelic group at id1018154 is indicated by “G” where $n=147$, while “A” represents the major allelic group where $n=173$. (B) “C” indicates the minor allelic group at id1014913 where $n=69$, and “T” represents the major allelic group where $n=263$.

Fig S5-18: (A-D) GWA analysis of fluorescence color classes CC.21 (A), CC.31 (B), CC.41 (C) and CC.52 (D) at day 1-14 after 90 mM NaCl. Red horizontal line indicates statistical significance ($p < 10^{-7}$).

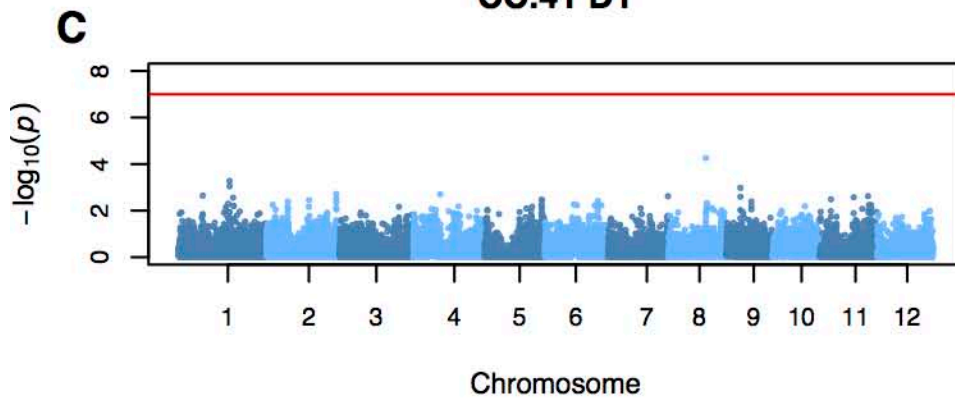
CC.21 D1



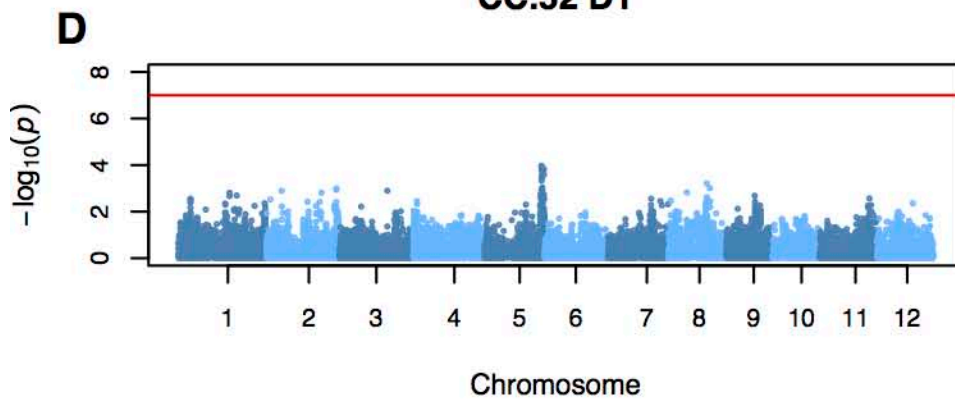
CC.31 D1



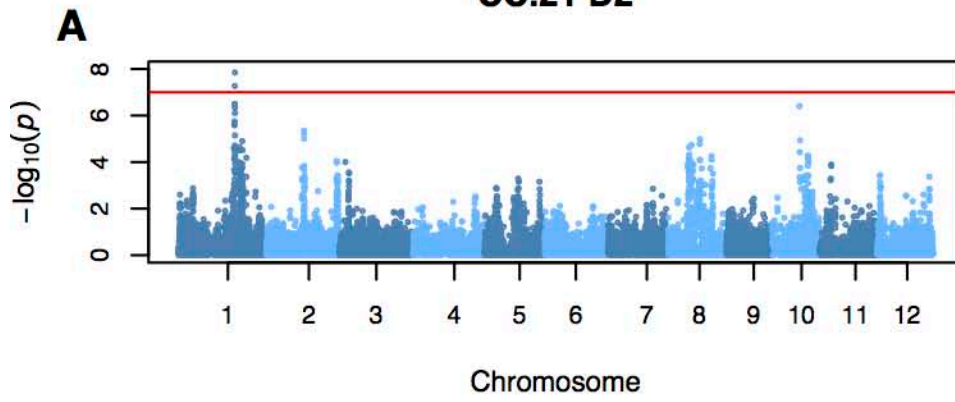
CC.41 D1



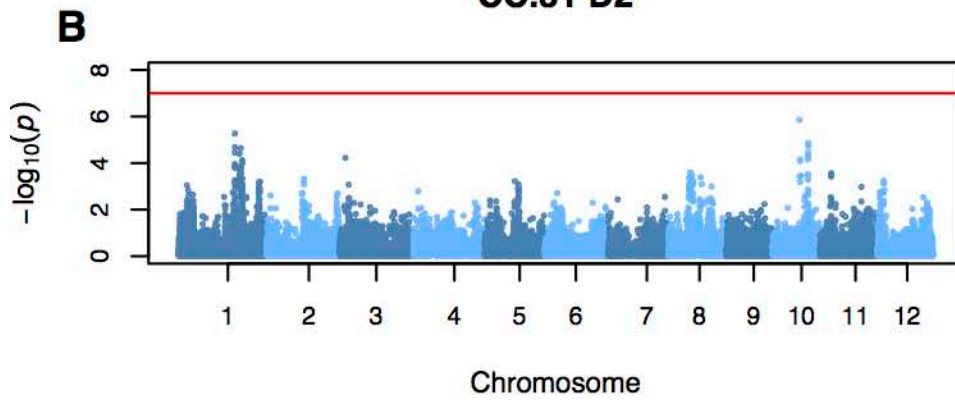
CC.52 D1



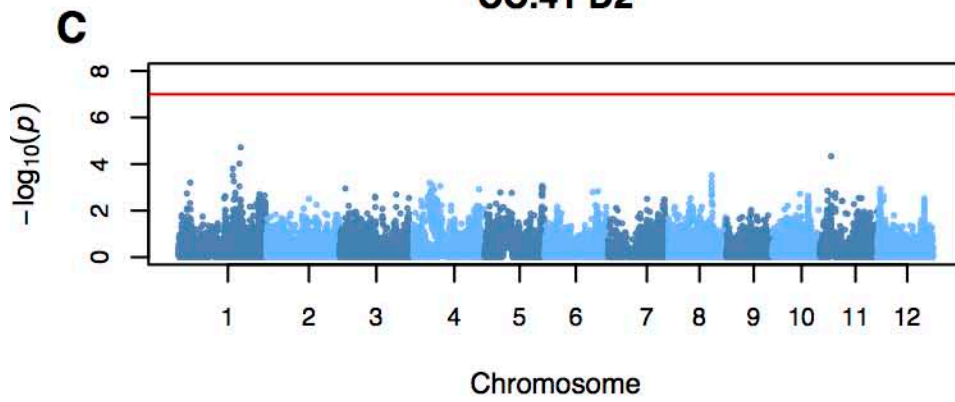
CC.21 D2



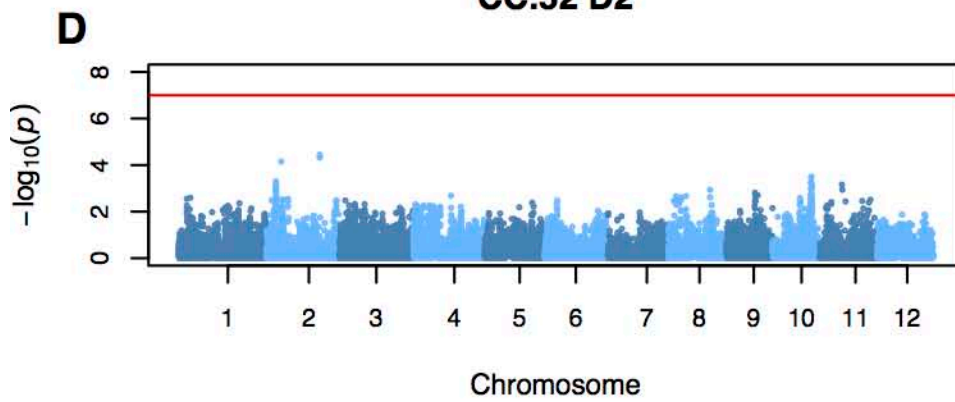
CC.31 D2



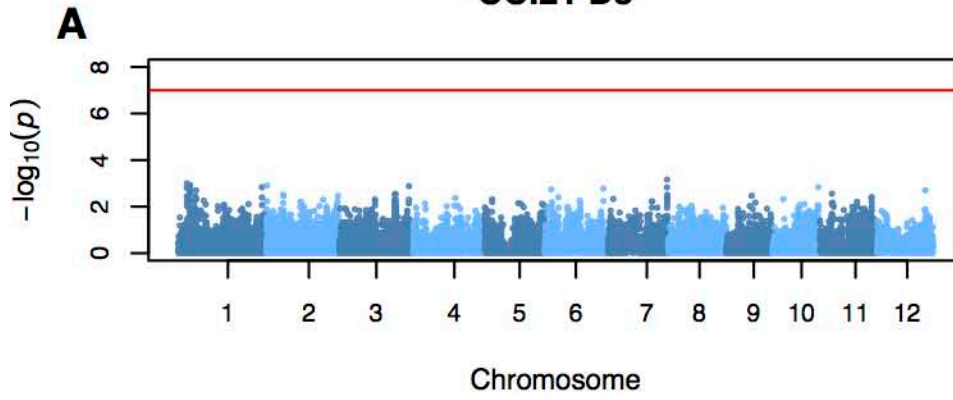
CC.41 D2



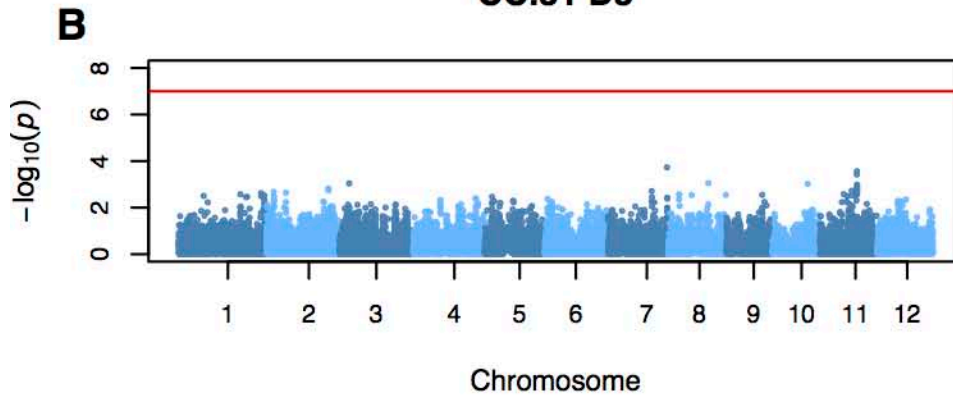
CC.52 D2



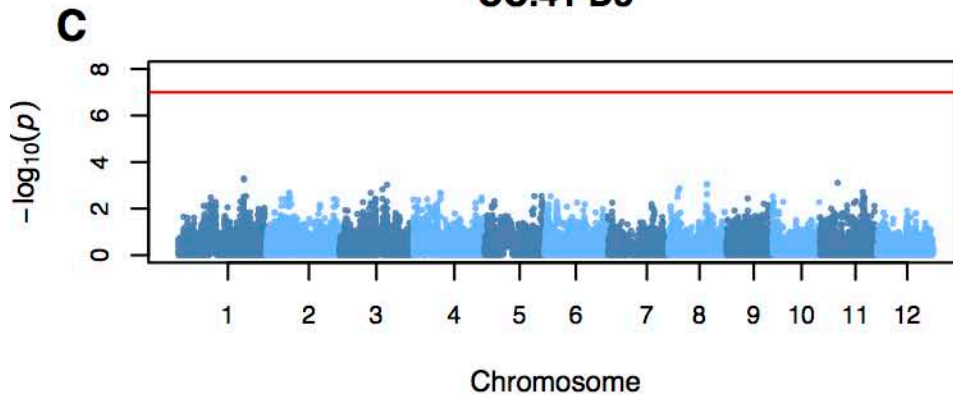
CC.21 D3



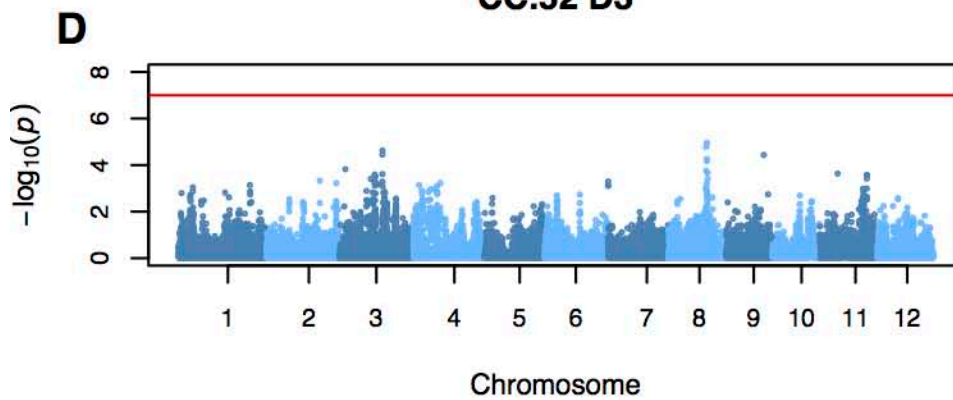
CC.31 D3



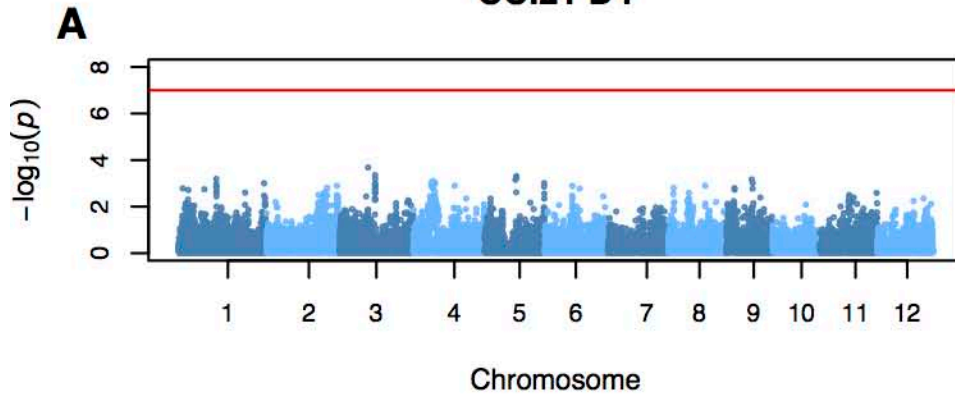
CC.41 D3



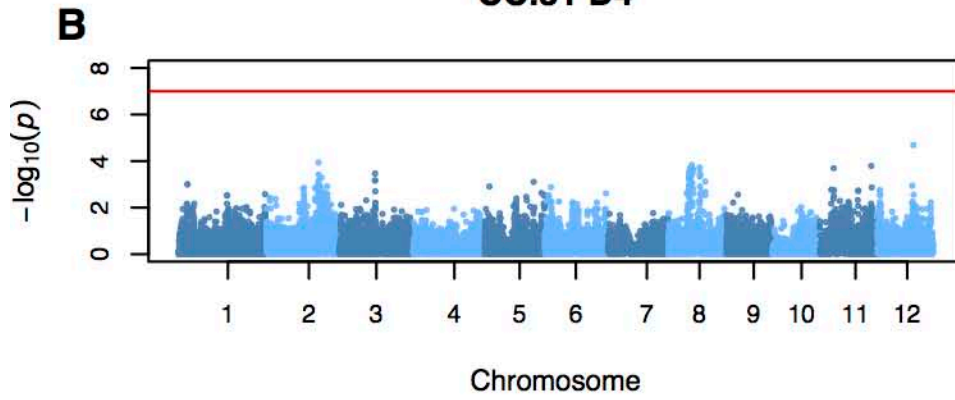
CC.52 D3



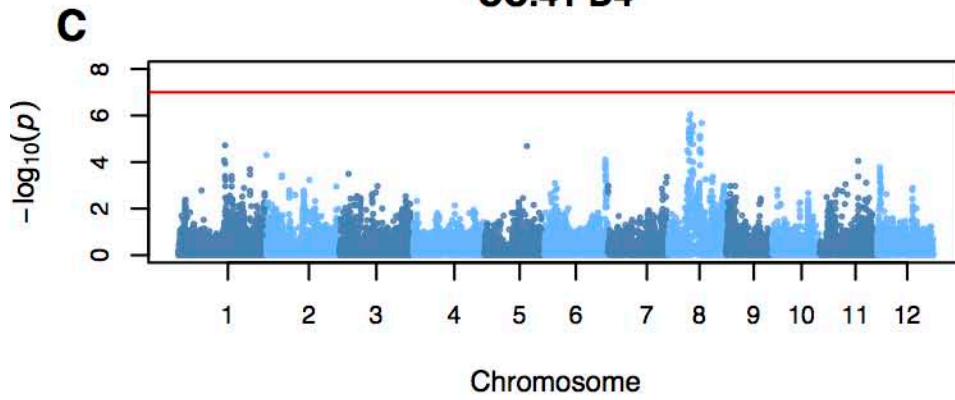
CC.21 D4



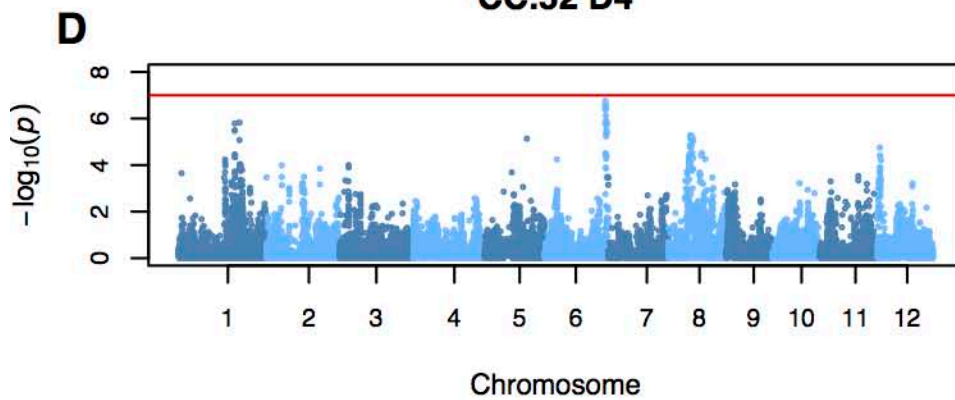
CC.31 D4



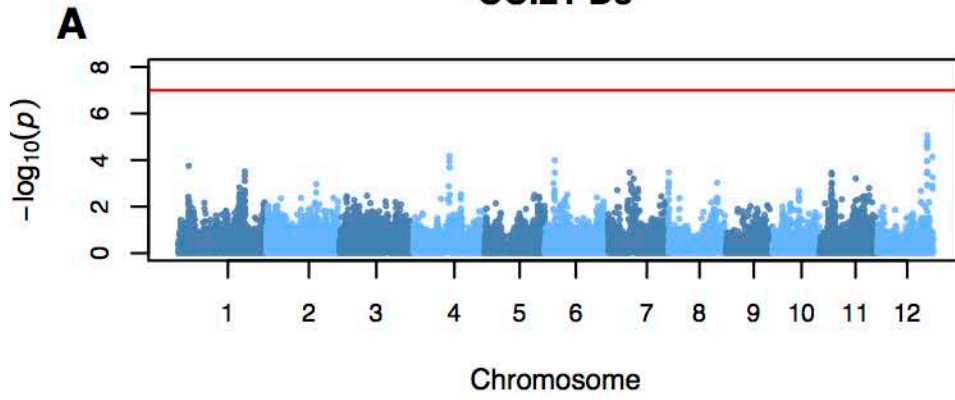
CC.41 D4



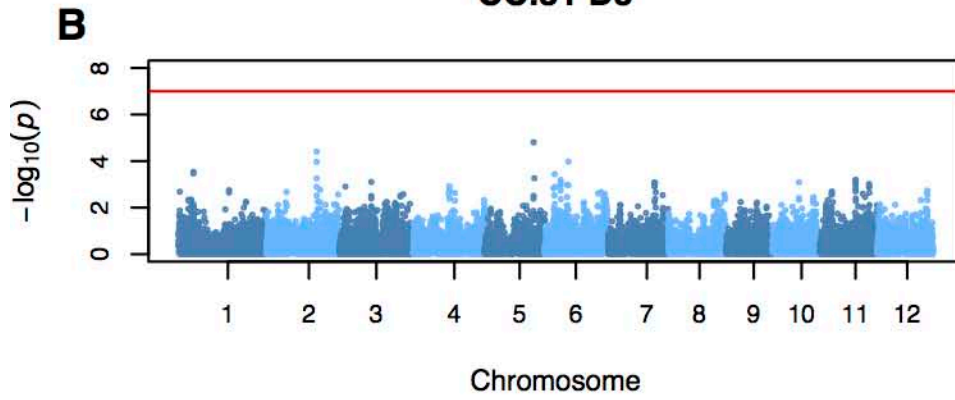
CC.52 D4



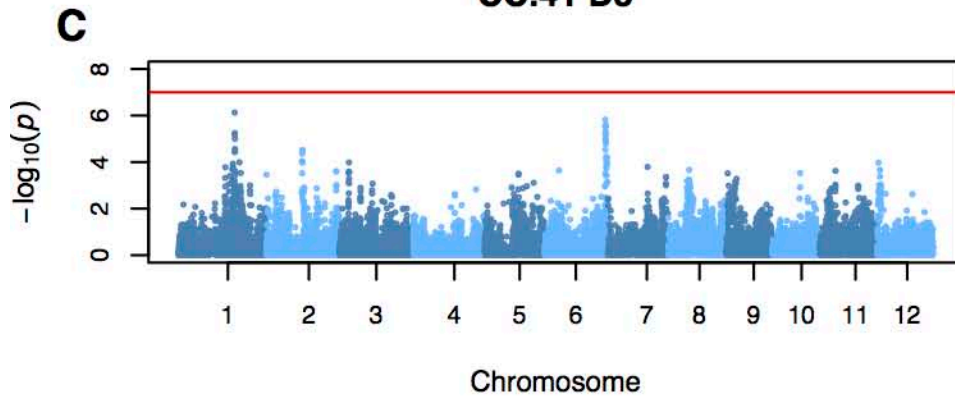
CC.21 D5



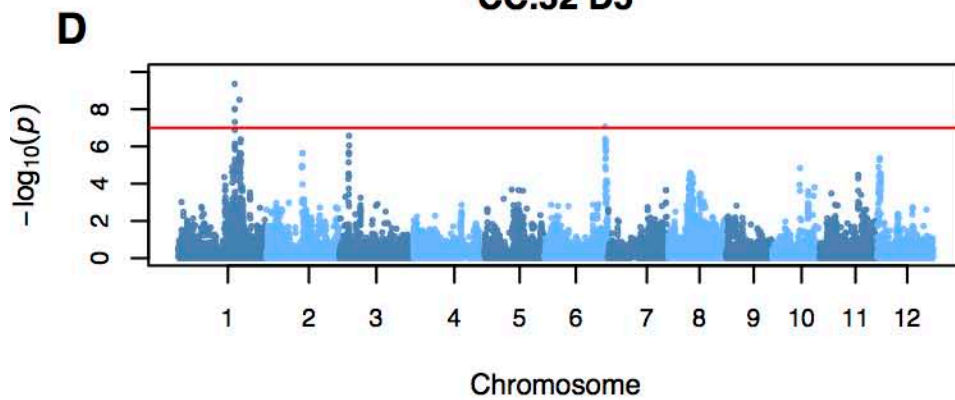
CC.31 D5



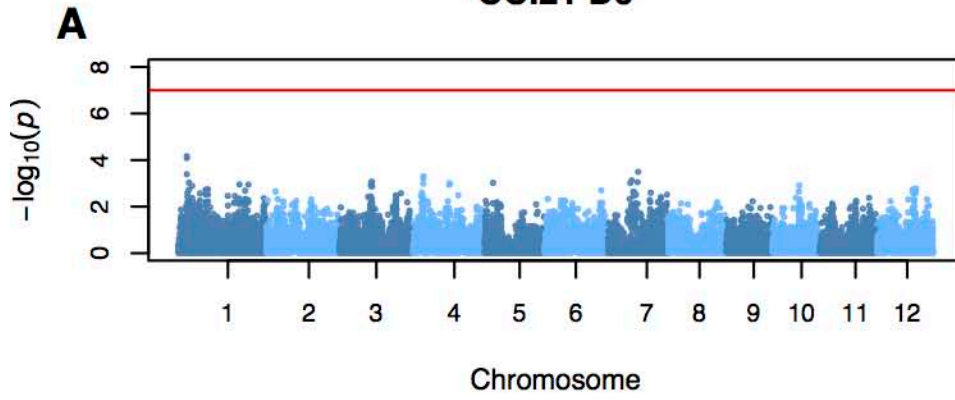
CC.41 D5



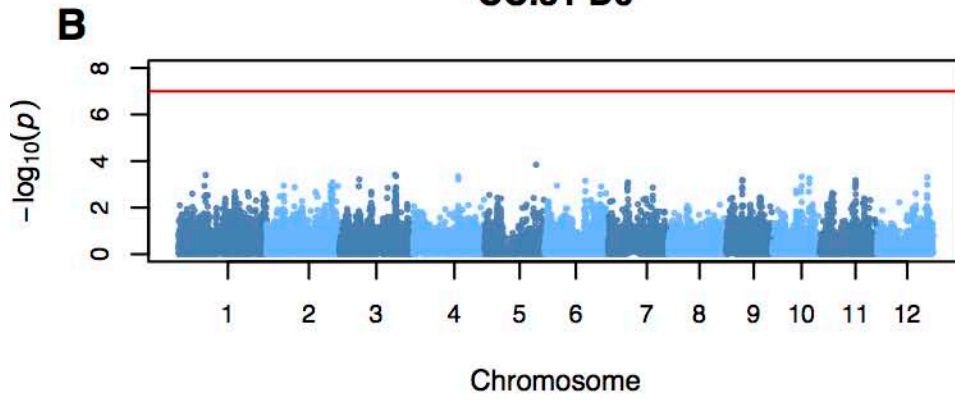
CC.52 D5



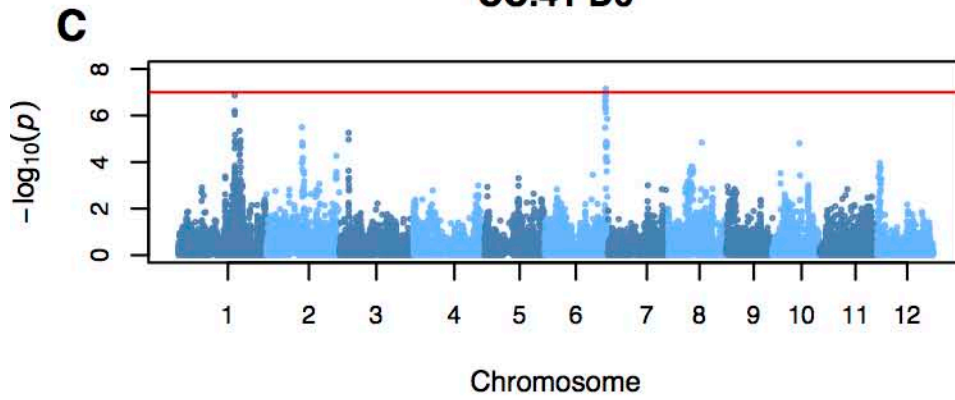
CC.21 D6



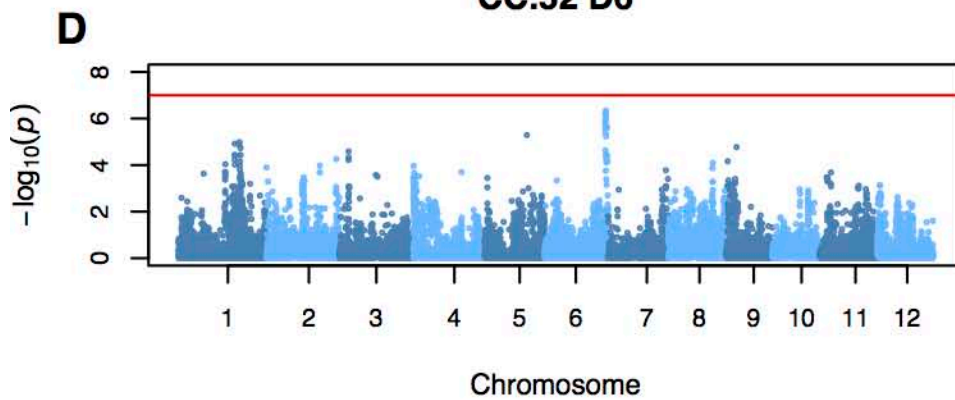
CC.31 D6



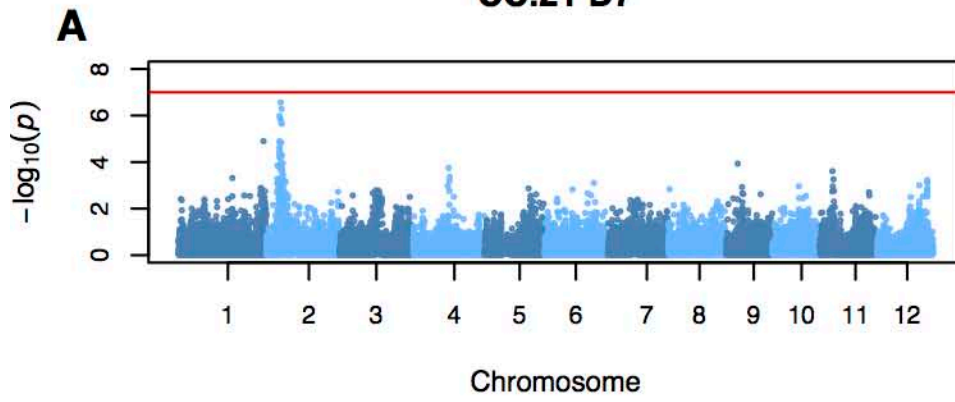
CC.41 D6



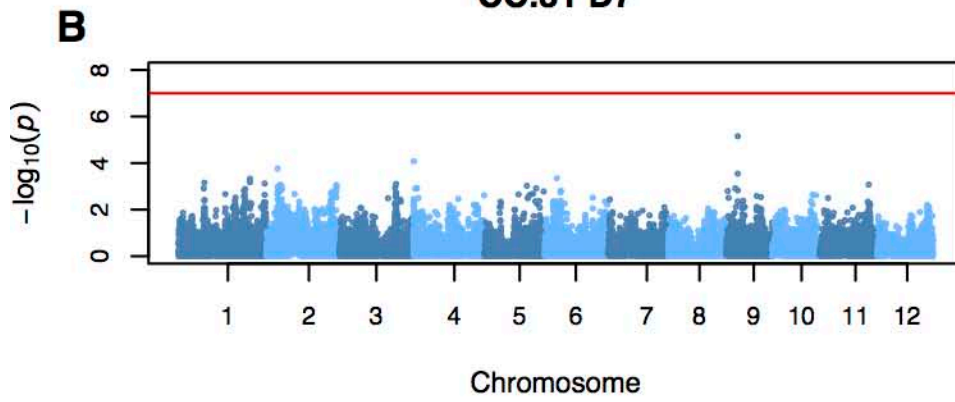
CC.52 D6



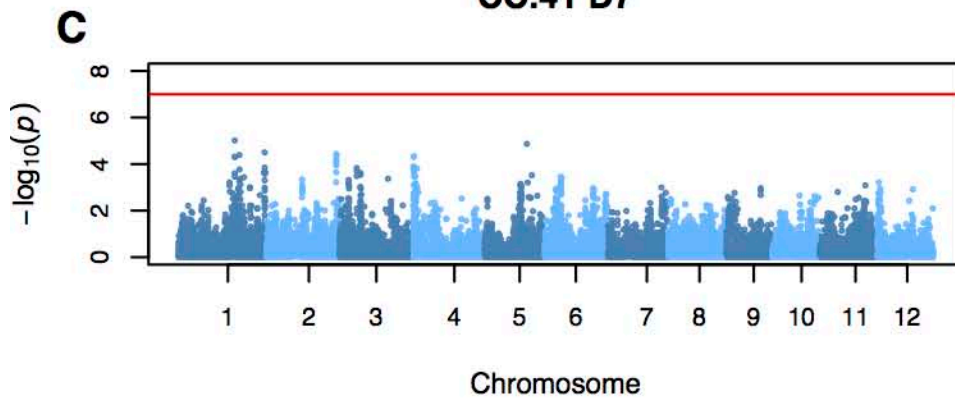
CC.21 D7



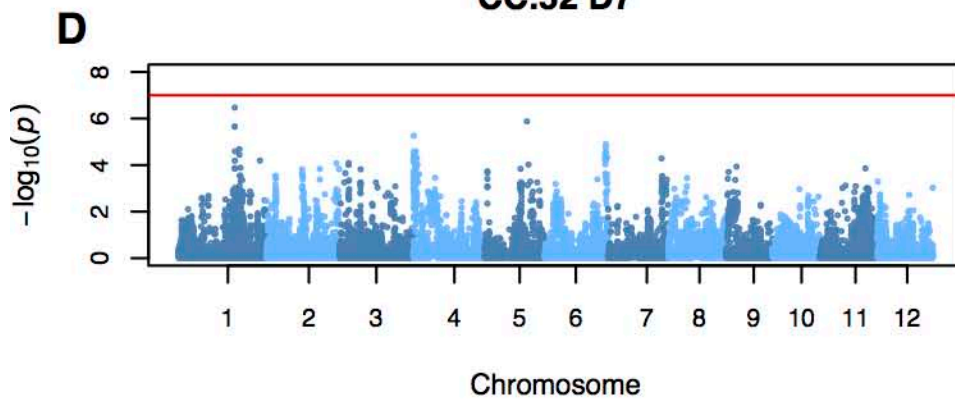
CC.31 D7



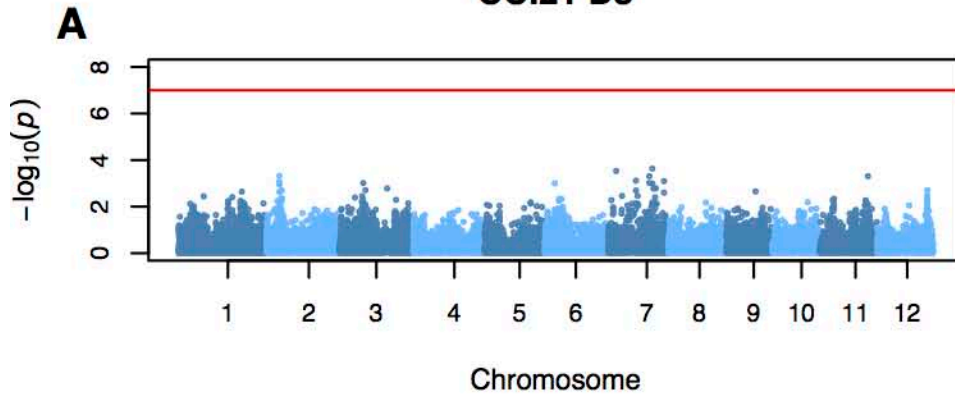
CC.41 D7



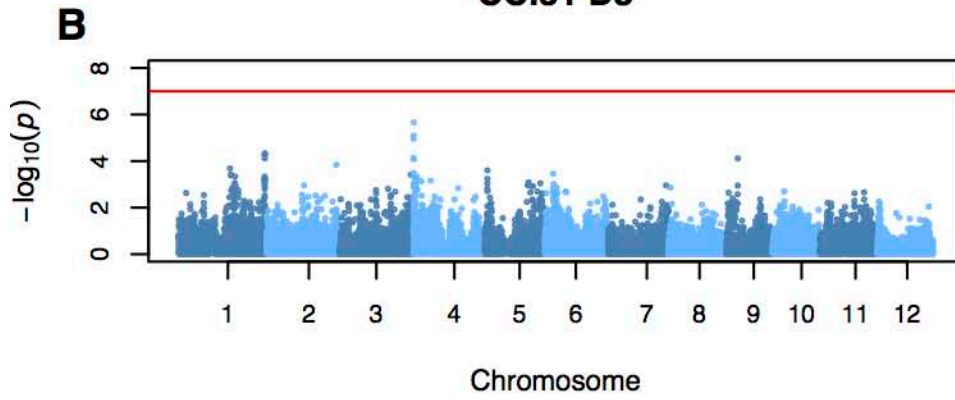
CC.52 D7



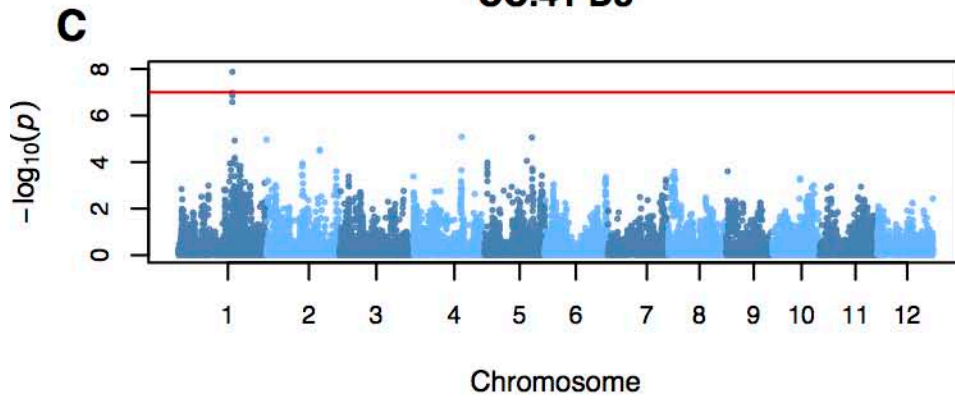
CC.21 D8



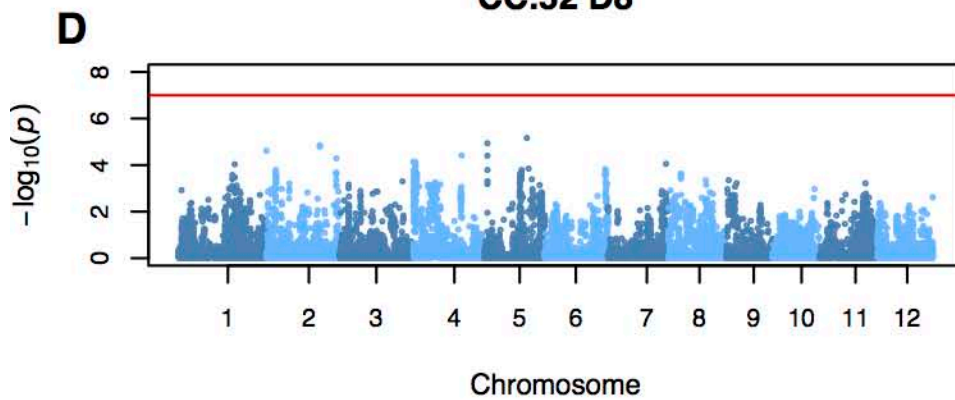
CC.31 D8



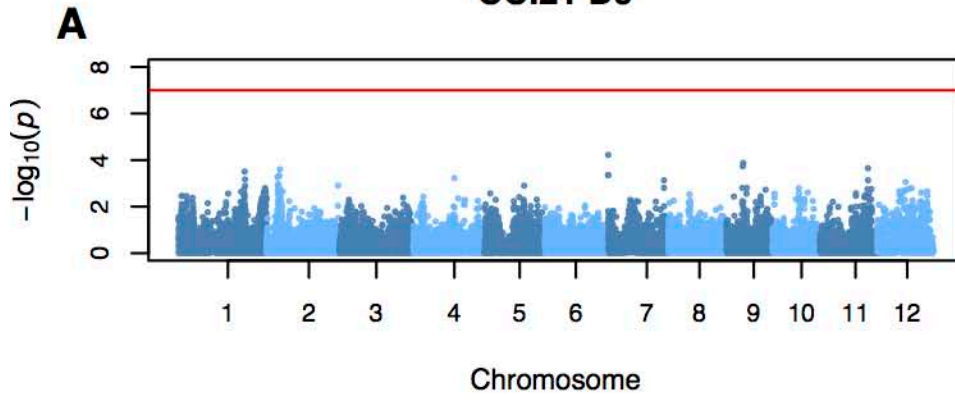
CC.41 D8



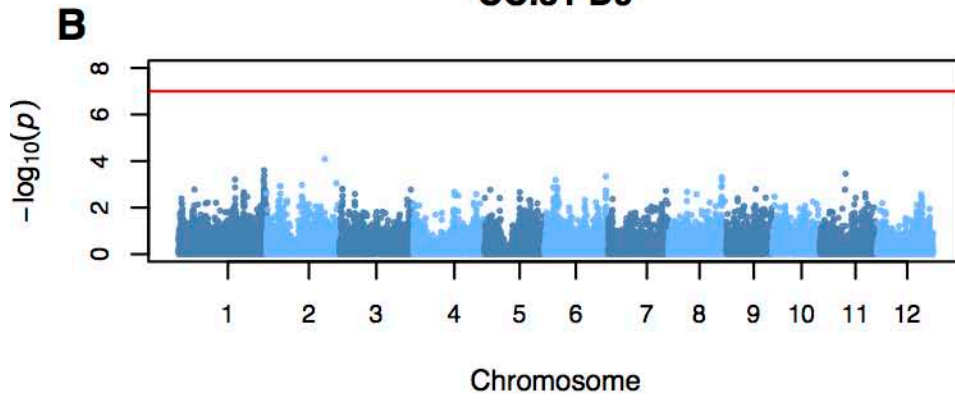
CC.52 D8



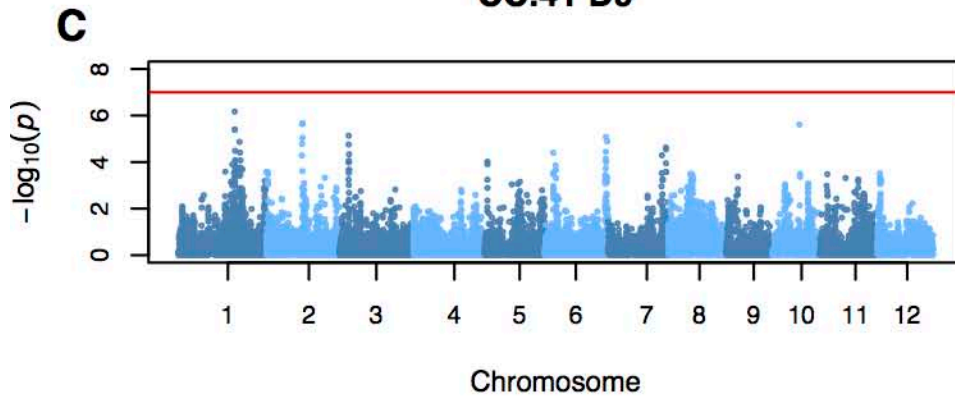
CC.21 D9



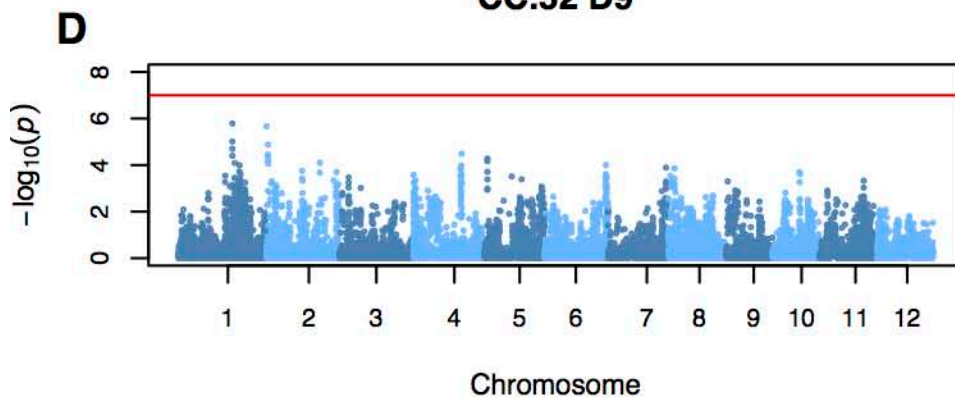
CC.31 D9



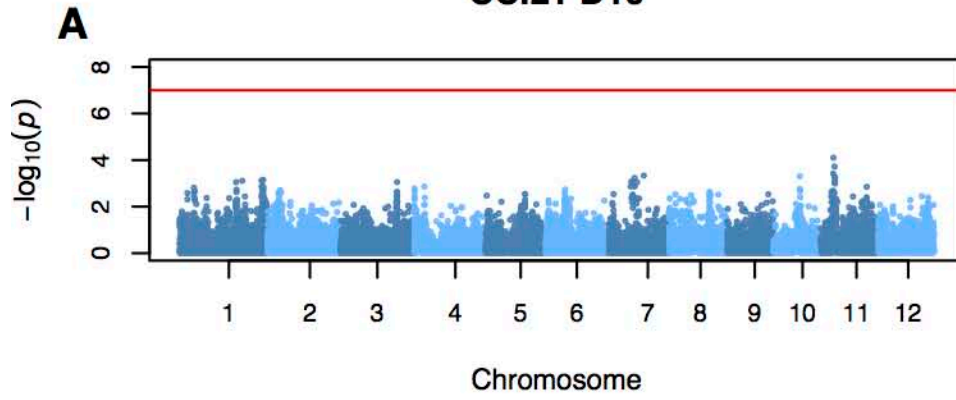
CC.41 D9



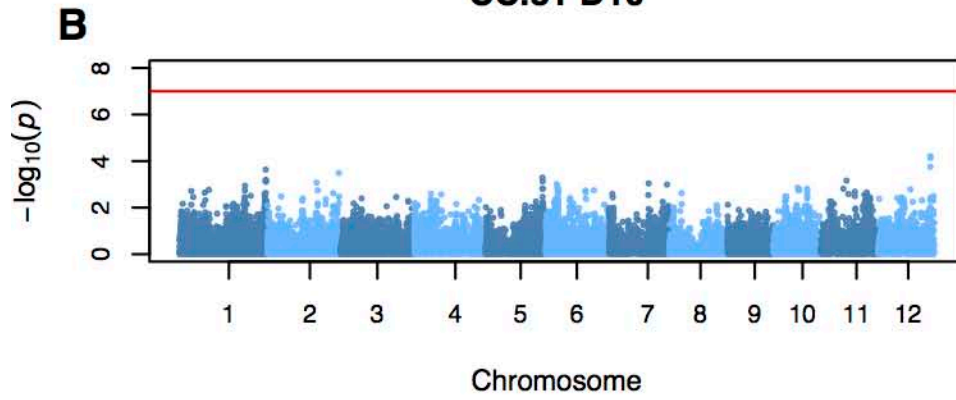
CC.52 D9



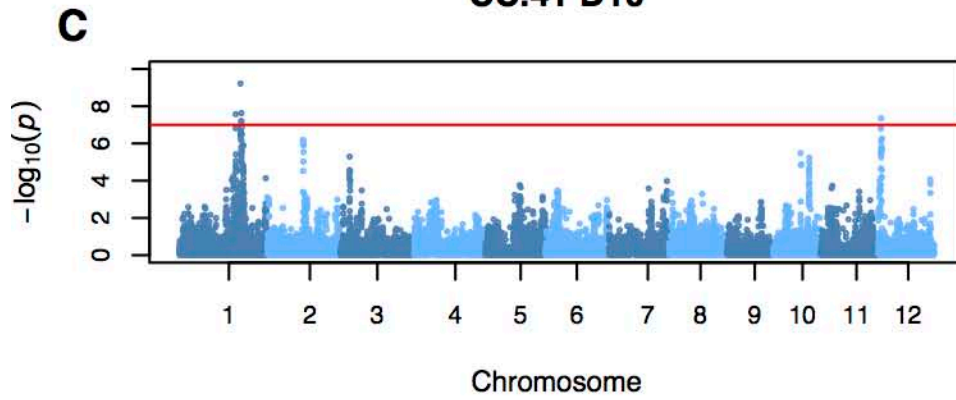
CC.21 D10



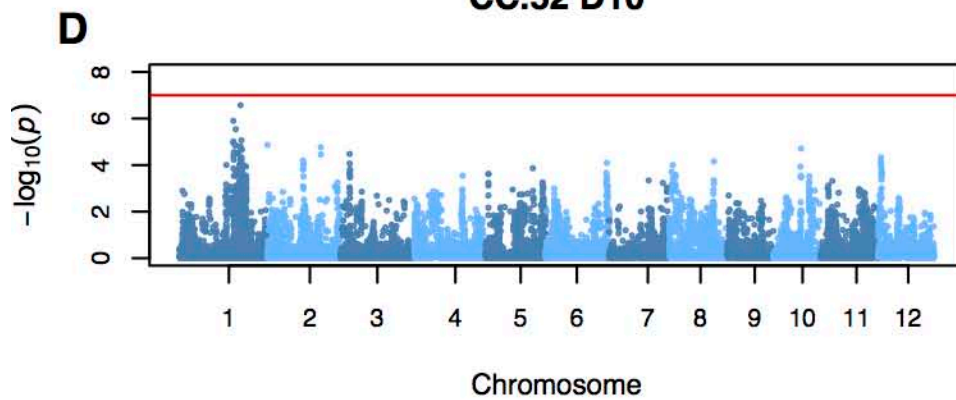
CC.31 D10



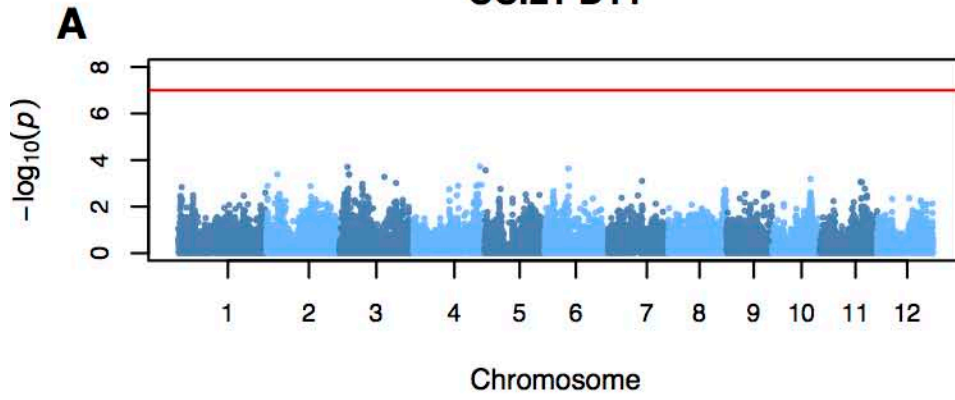
CC.41 D10



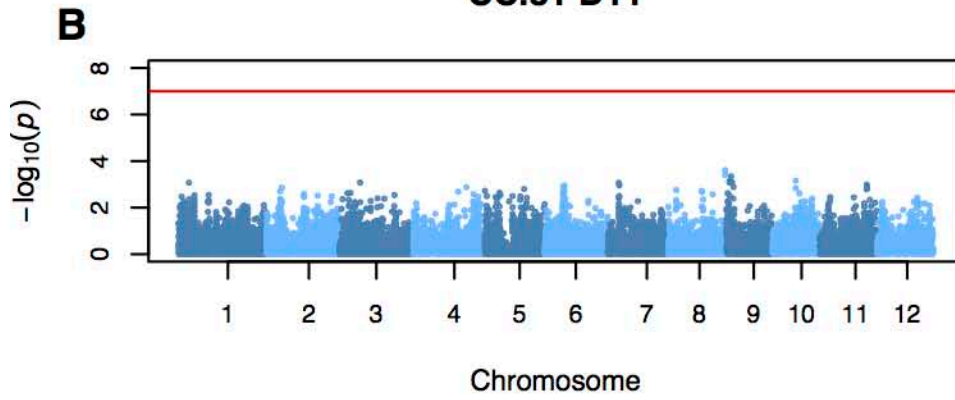
CC.52 D10



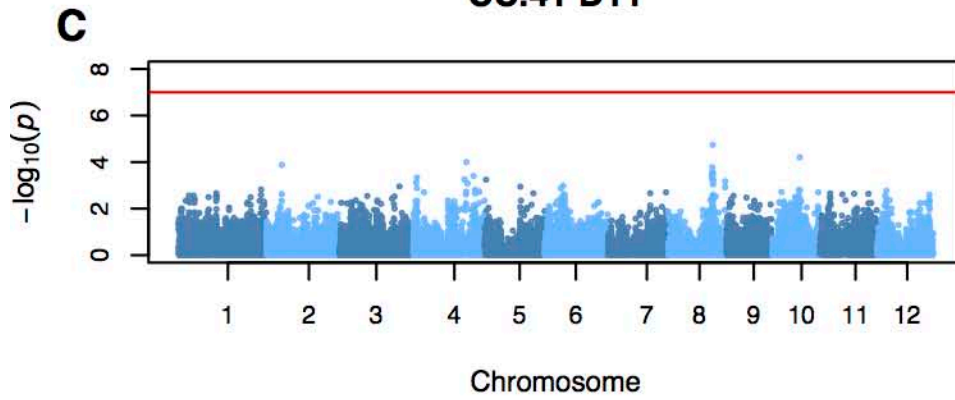
CC.21 D11



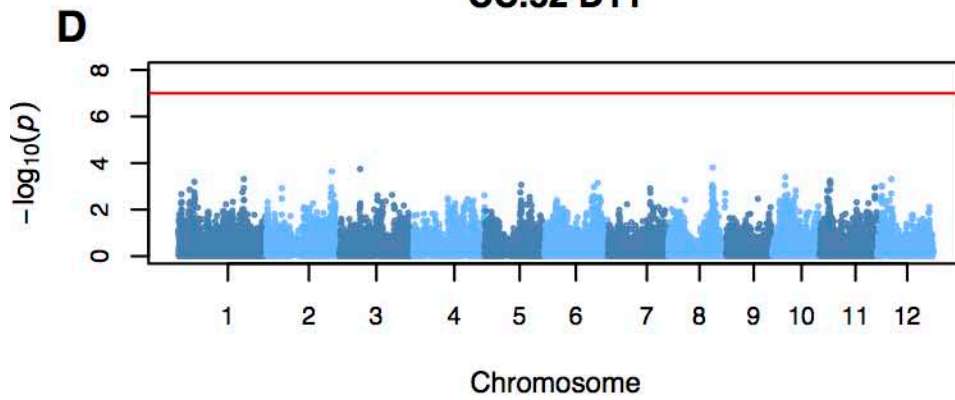
CC.31 D11



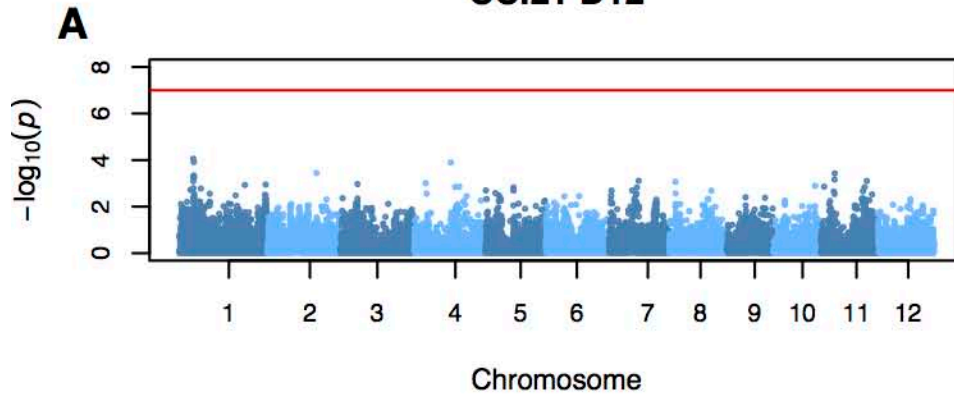
CC.41 D11



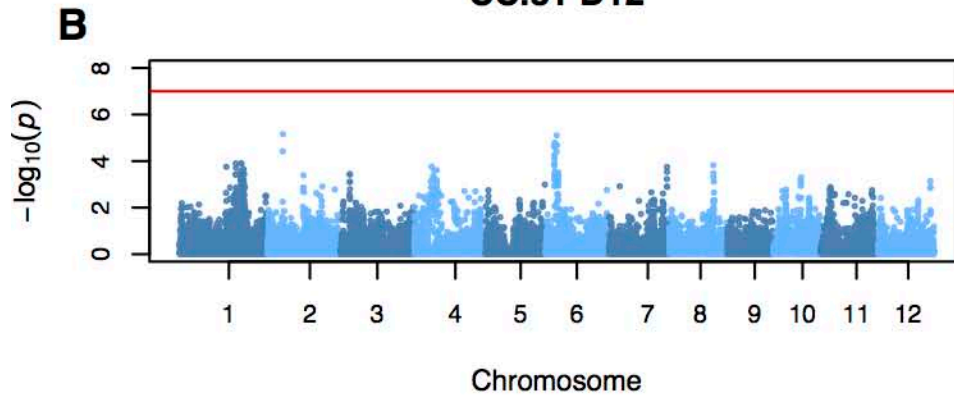
CC.52 D11



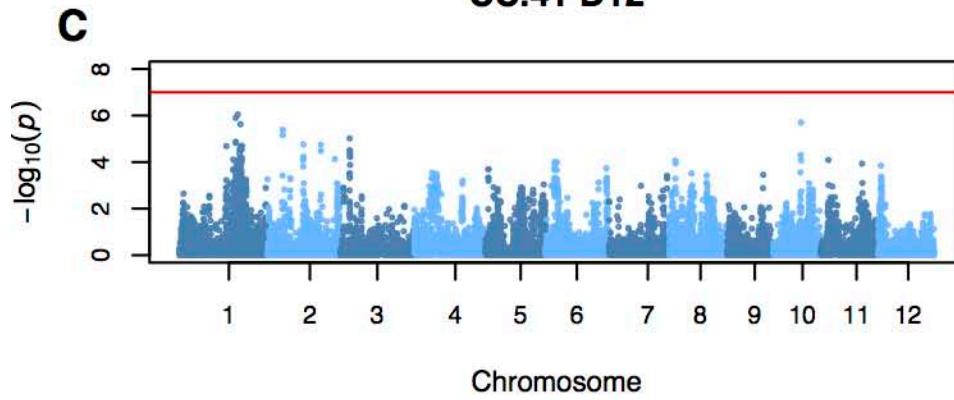
CC.21 D12



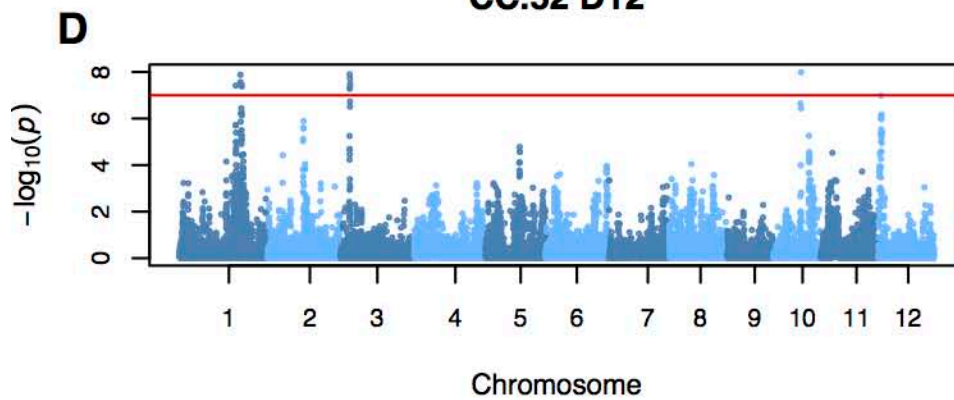
CC.31 D12



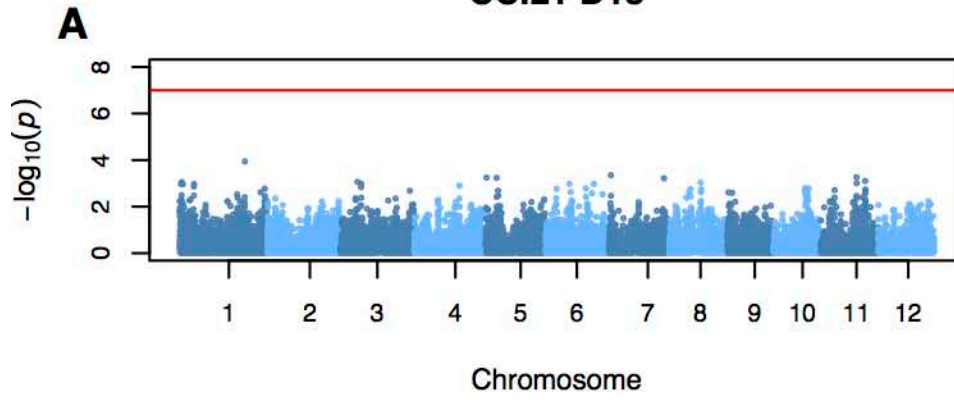
CC.41 D12



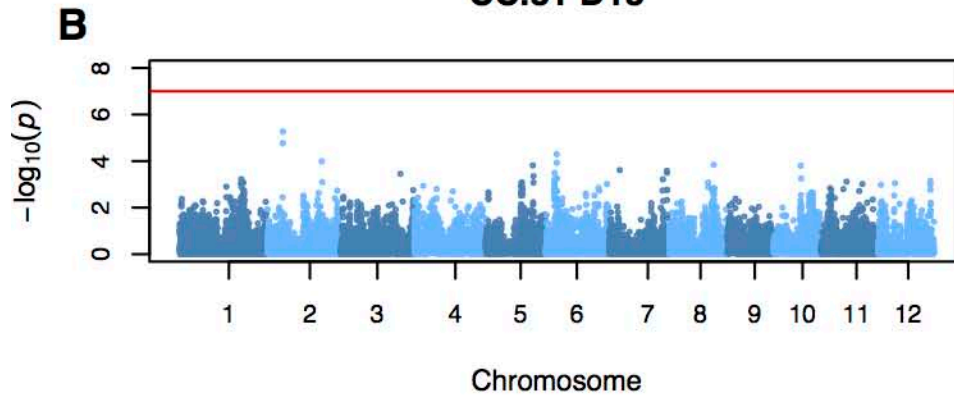
CC.52 D12



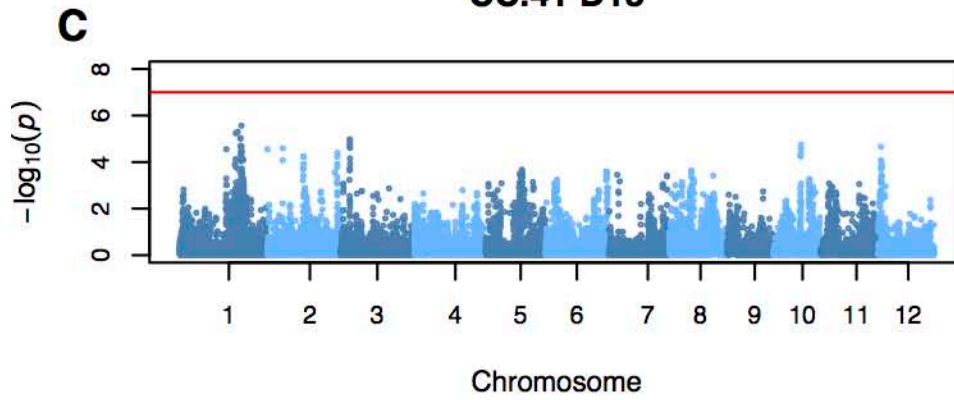
CC.21 D13



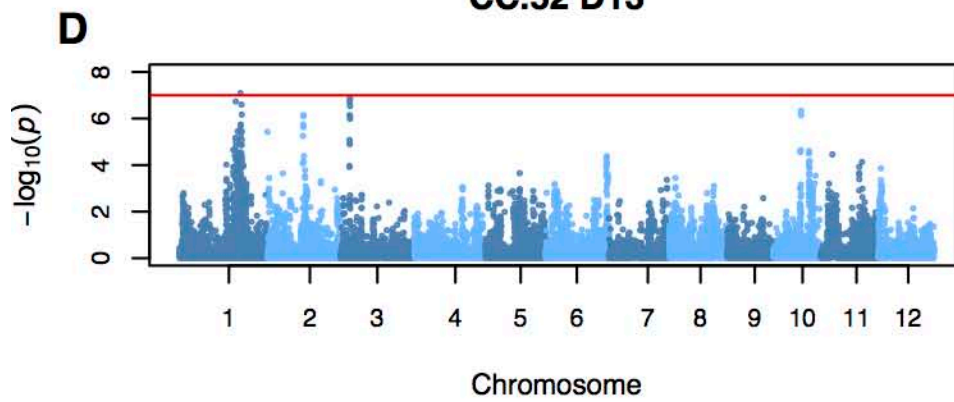
CC.31 D13



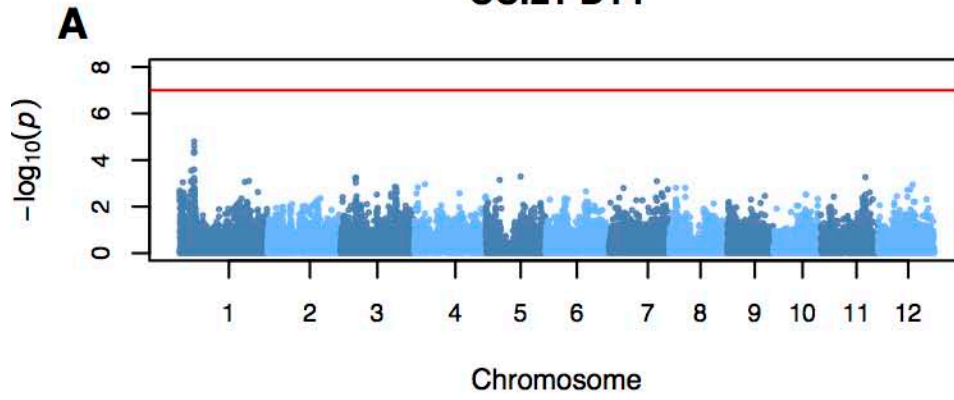
CC.41 D13



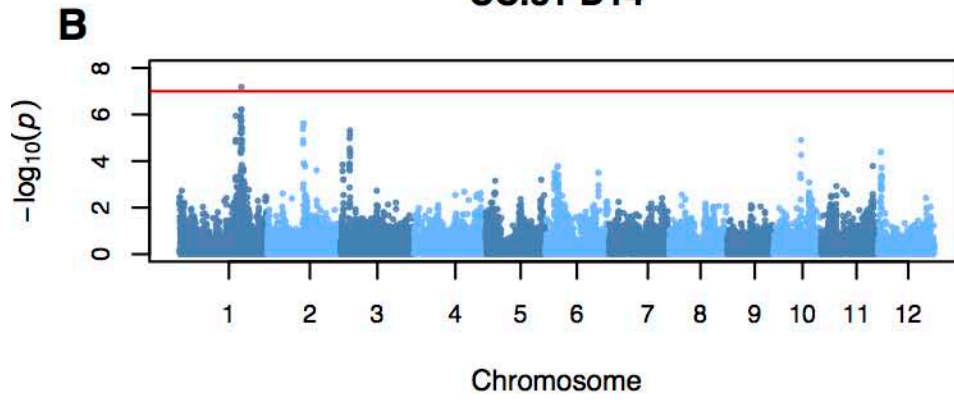
CC.52 D13



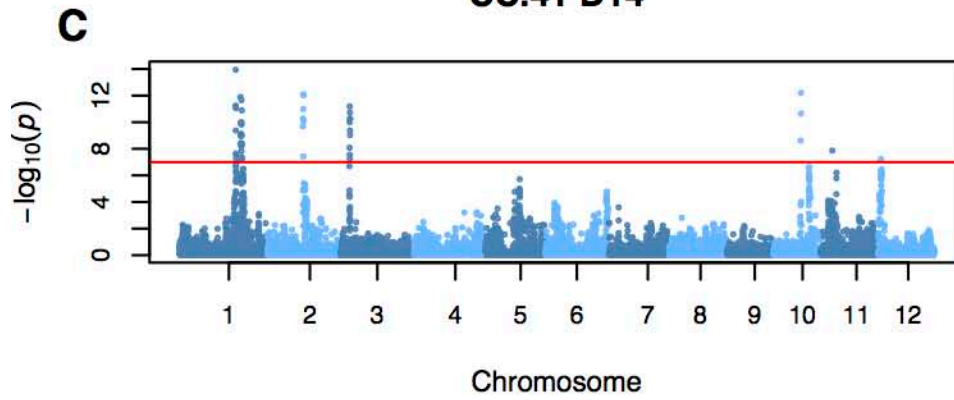
CC.21 D14



CC.31 D14



CC.41 D14



CC.52 D14

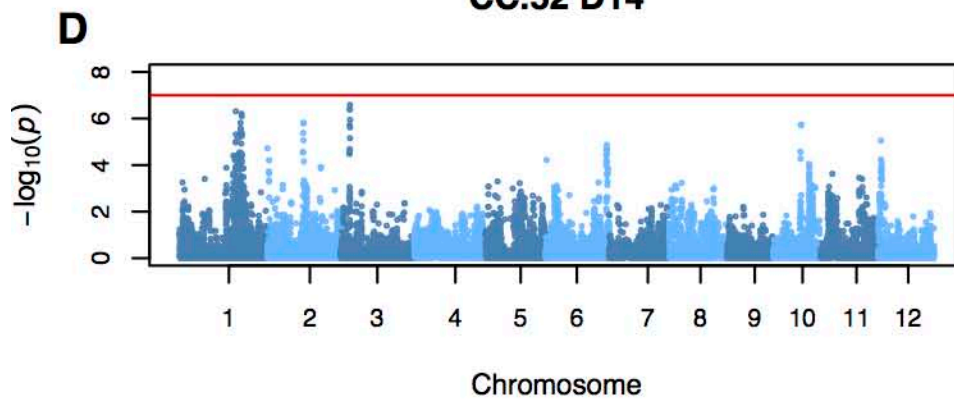
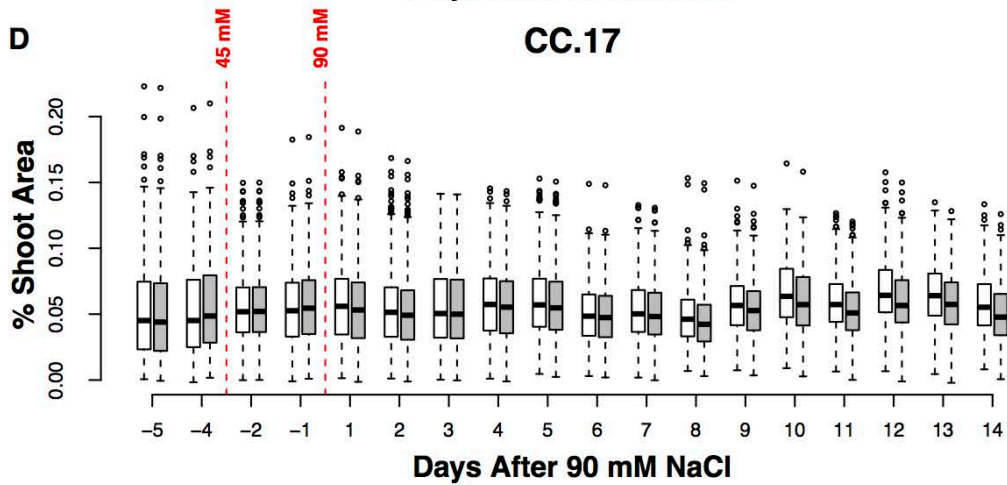
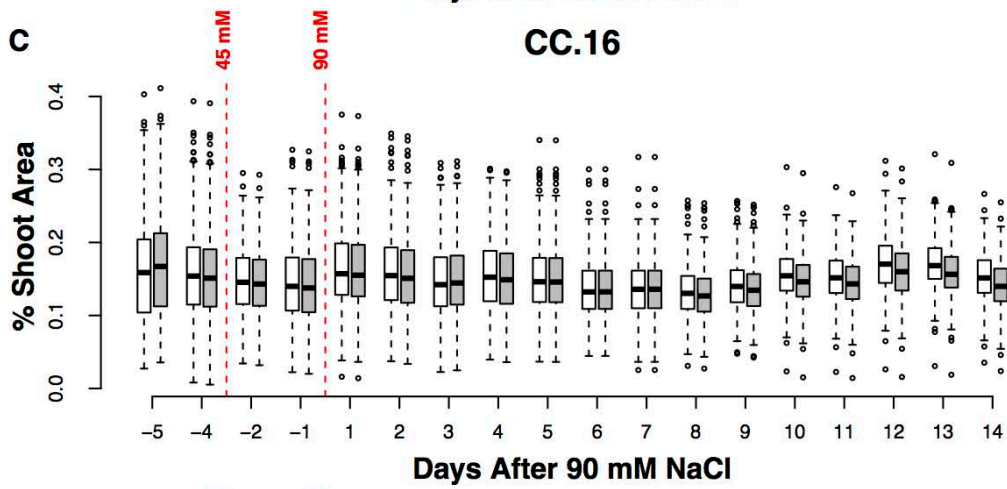
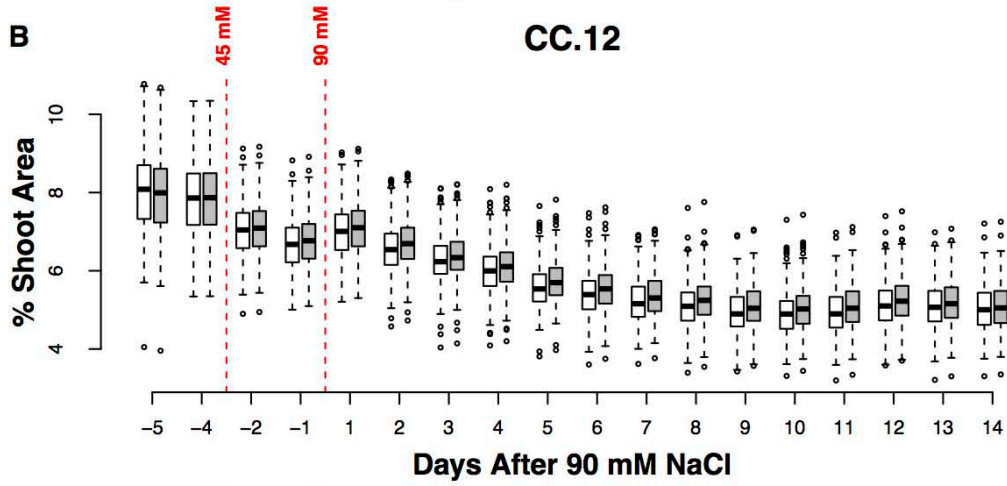
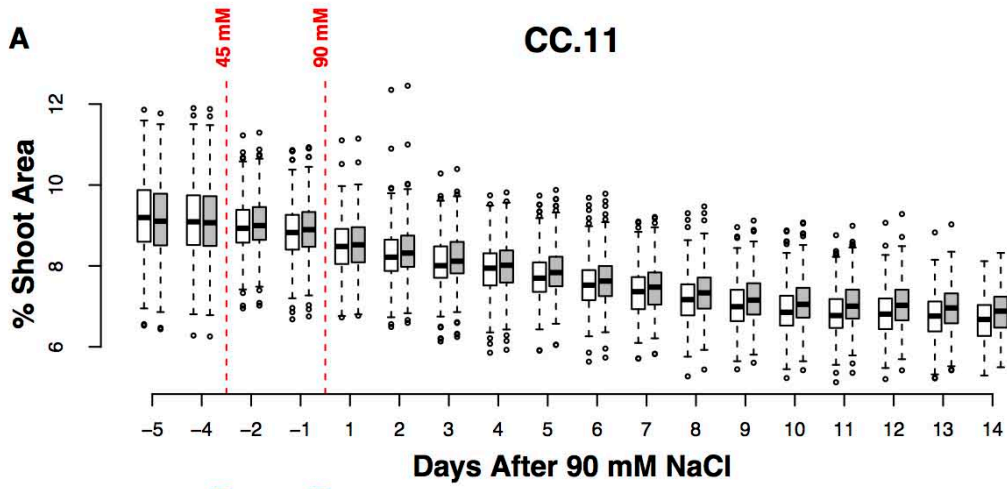
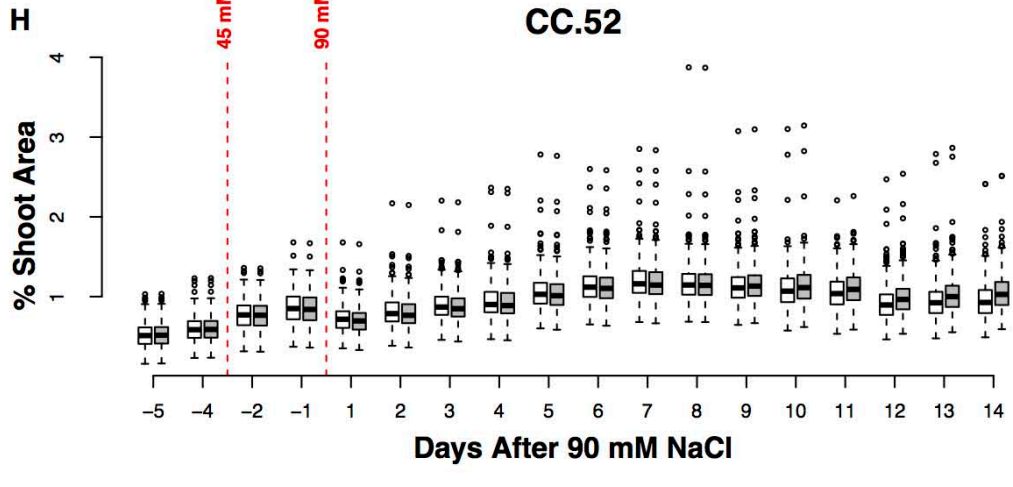
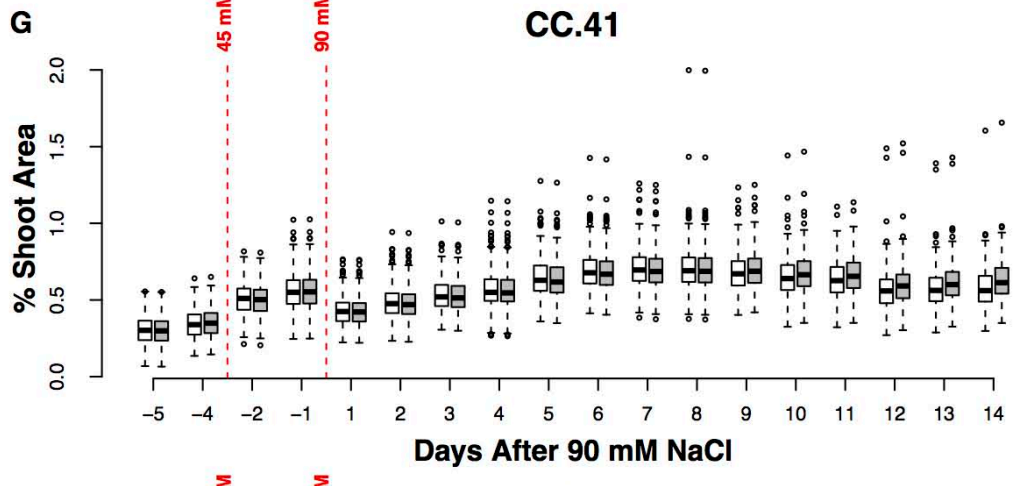
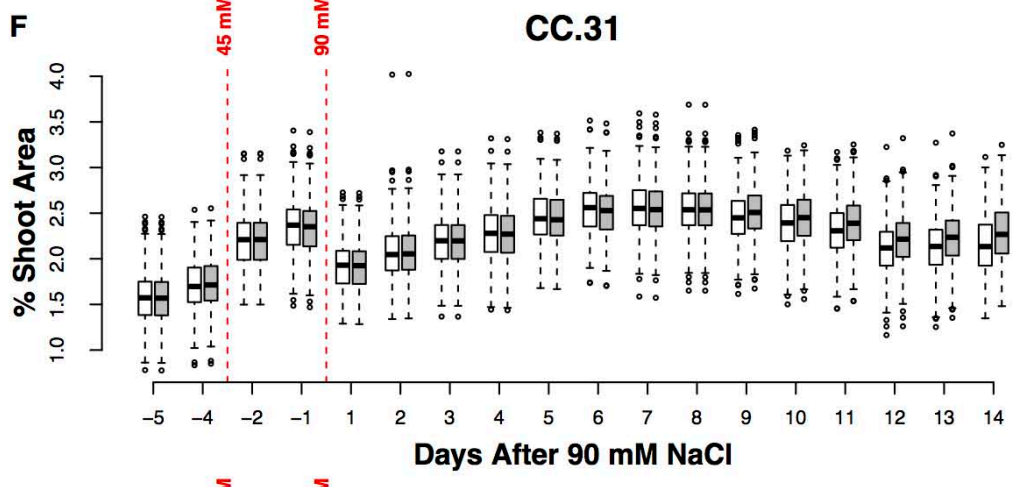
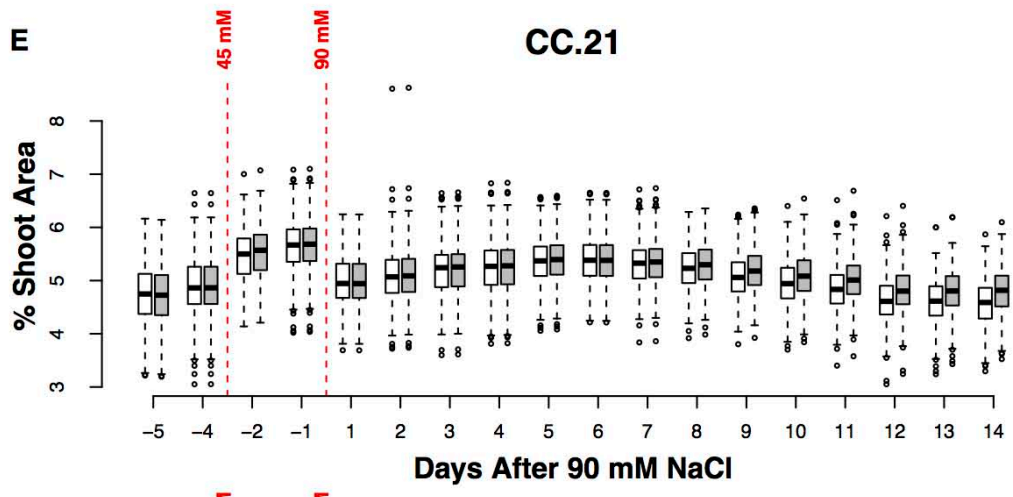
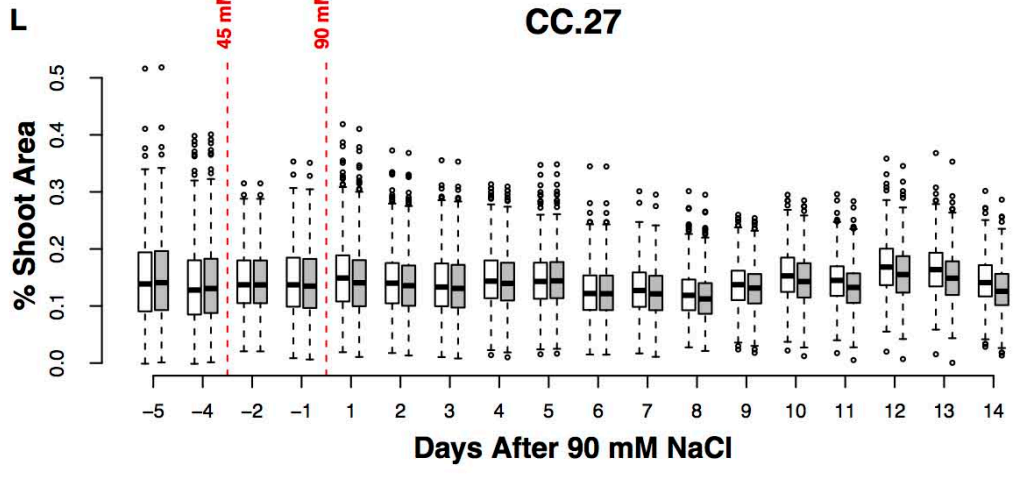
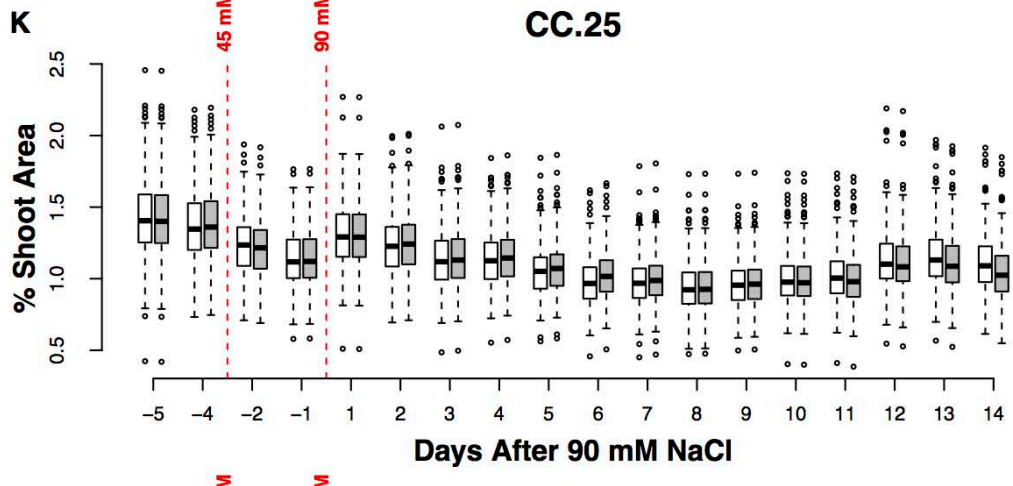
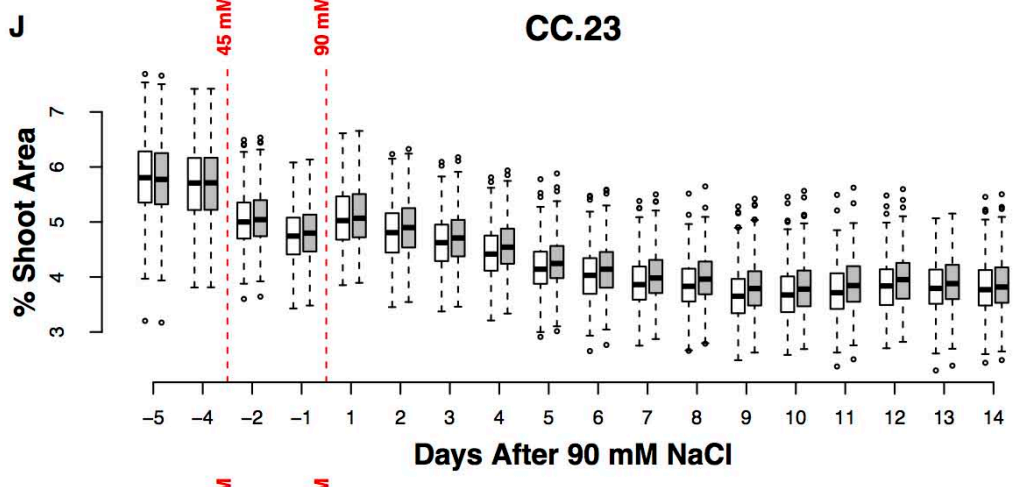
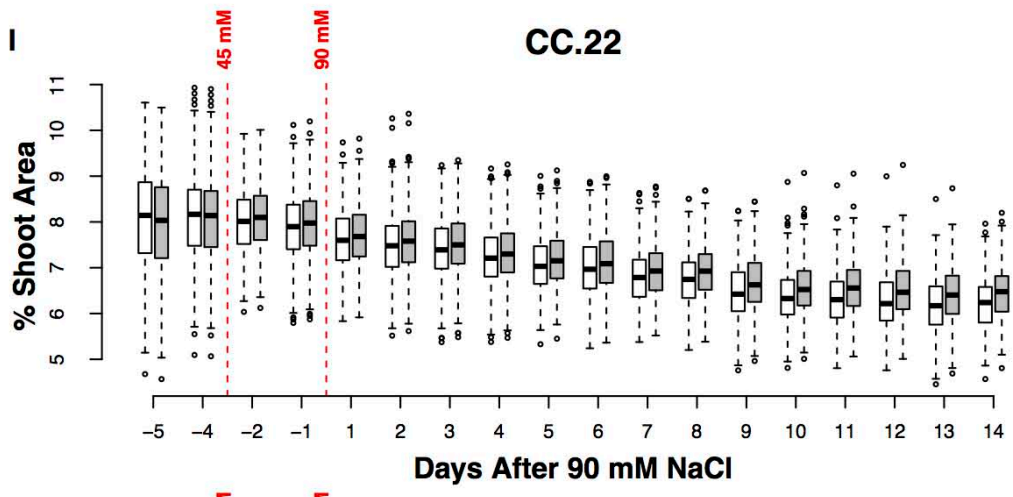
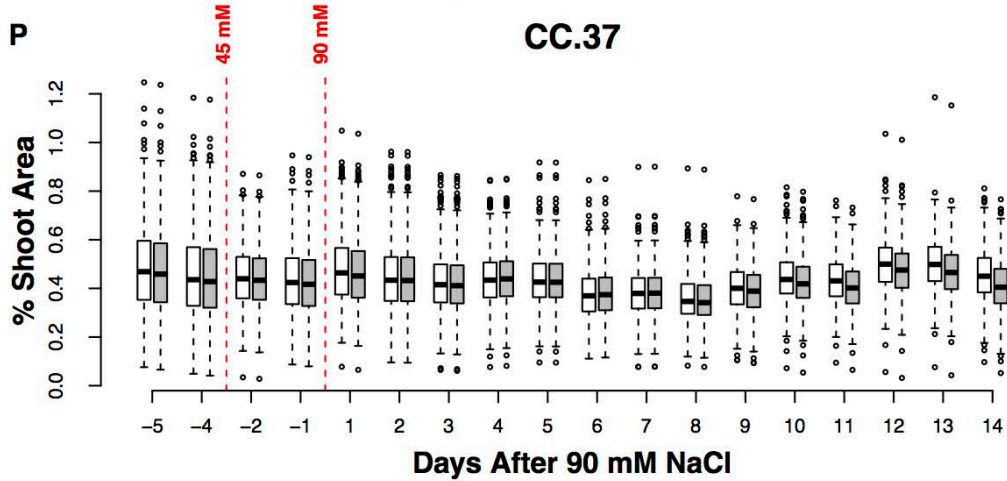
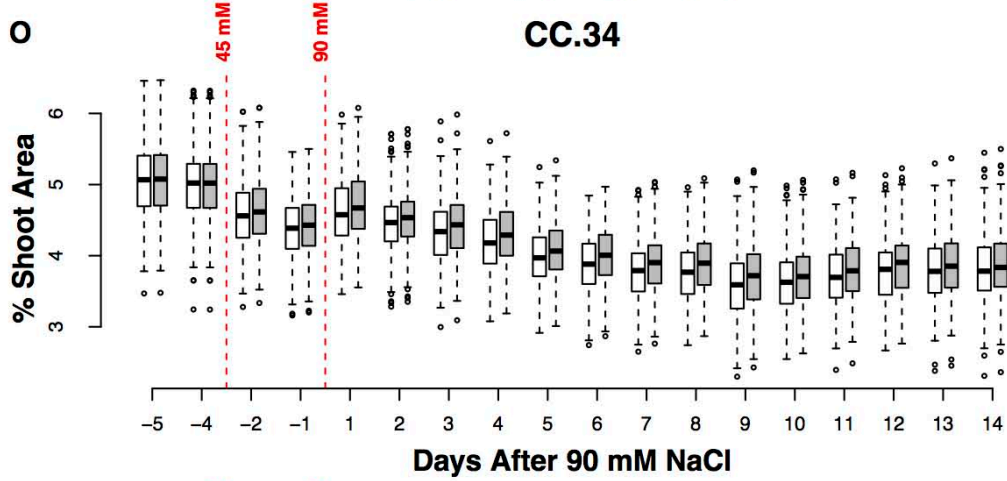
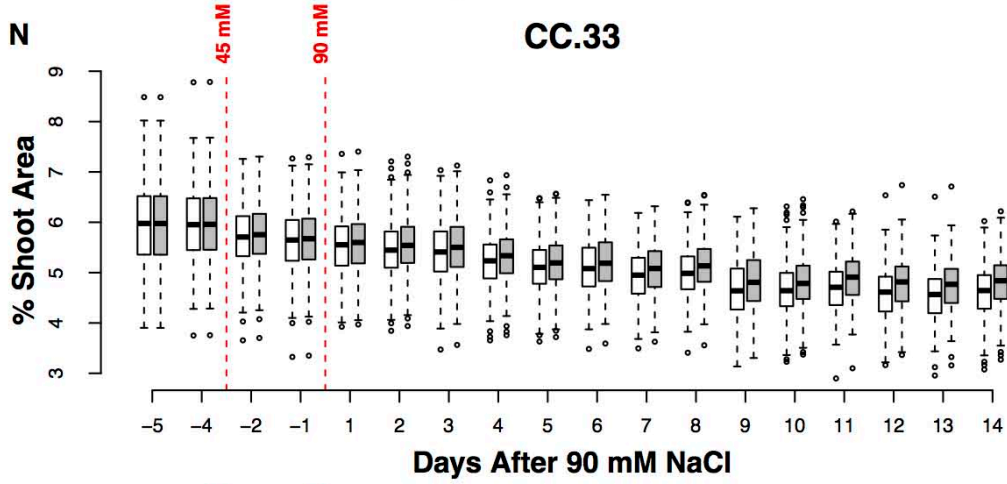
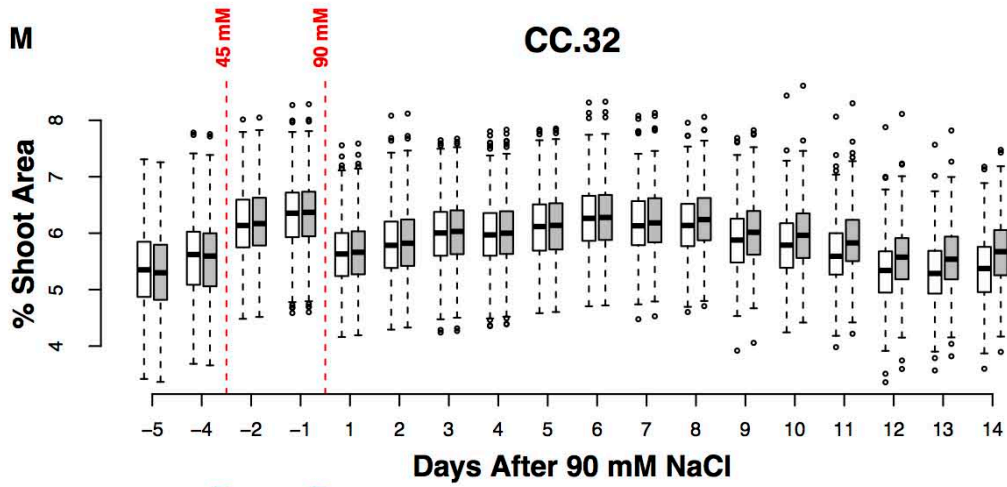


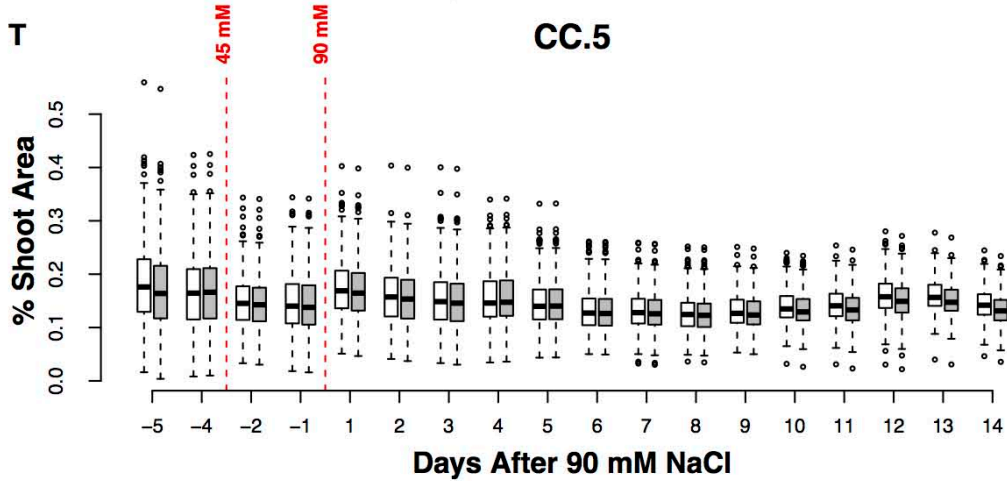
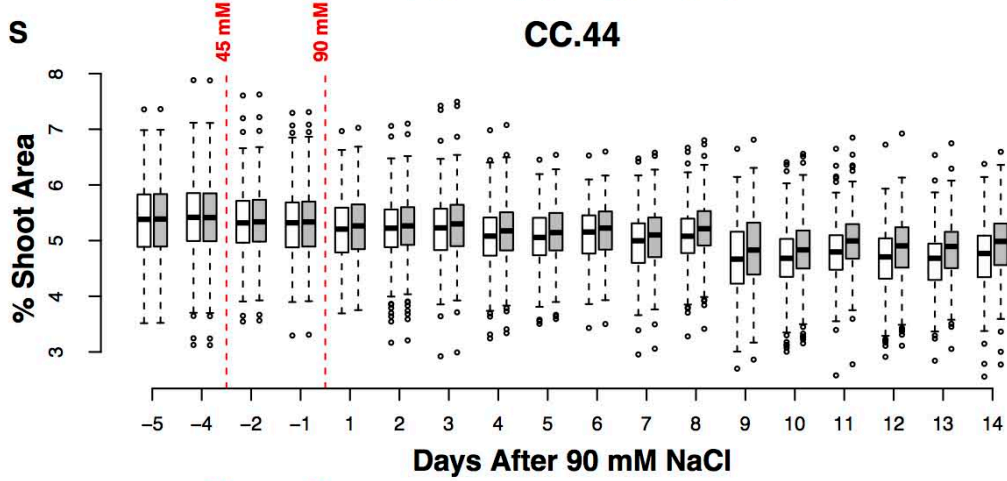
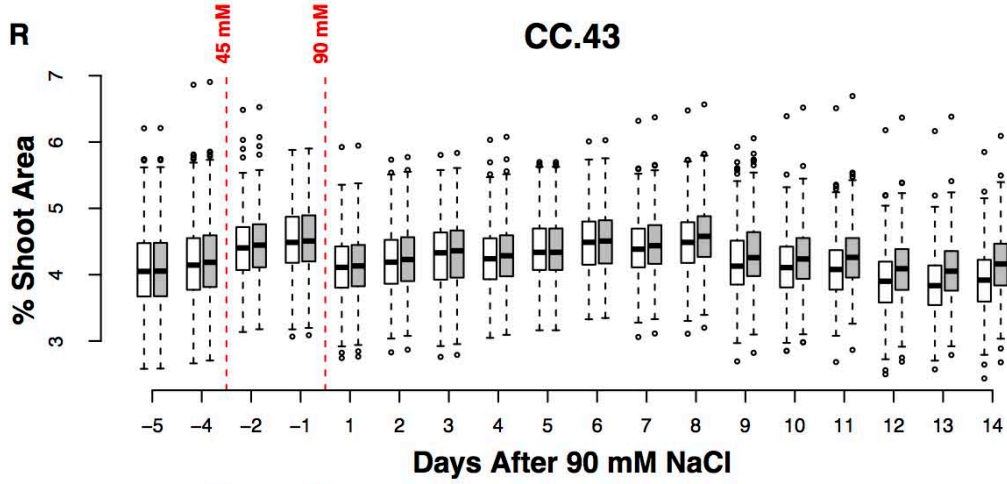
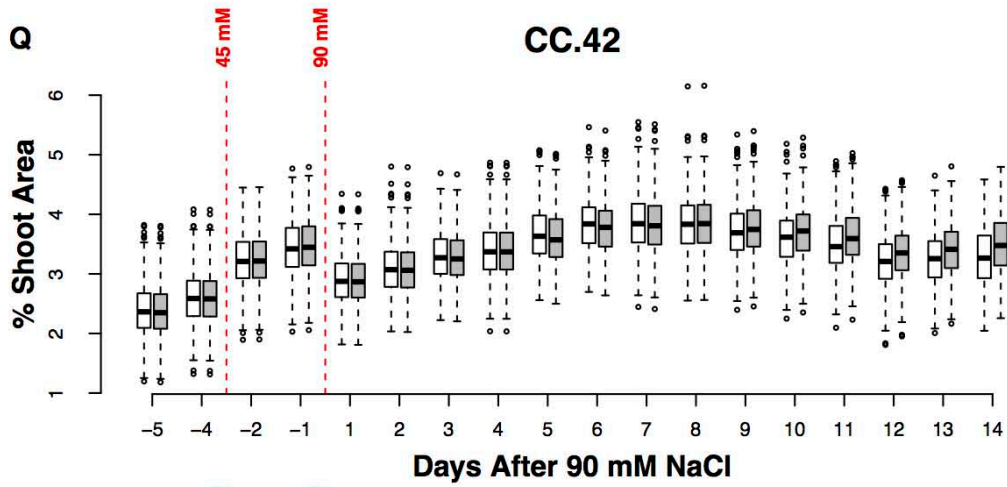
Fig S19: (A-AF) Trajectories of the 32 salinity-responsive fluorescence color classes. Control plants are indicated by white bars, while plants in saline conditions are indicated by grey bars. Values are expressed as a percentage of total pixels from two side view fluorescence images.

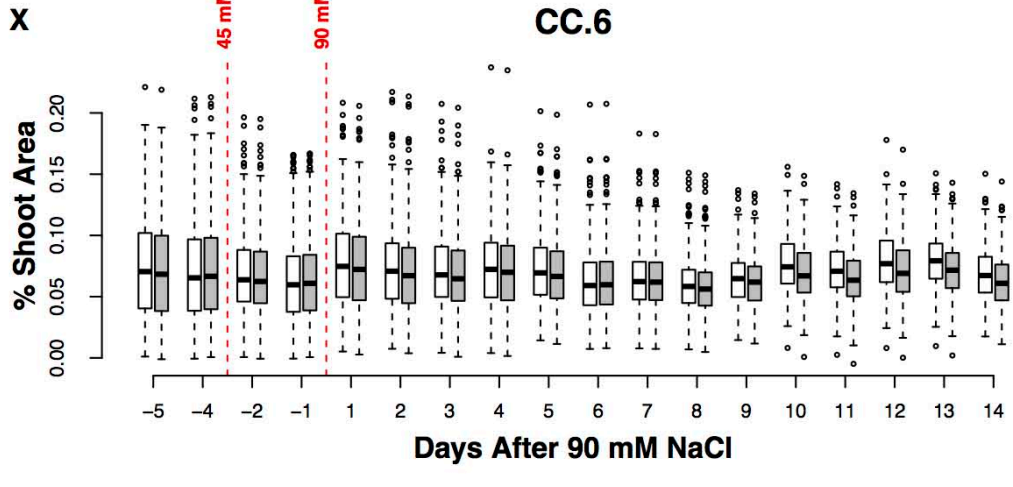
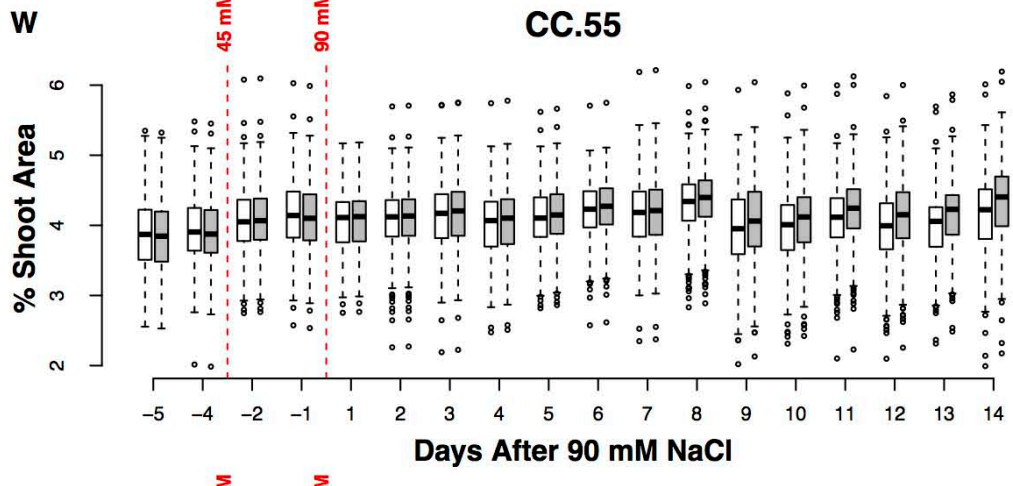
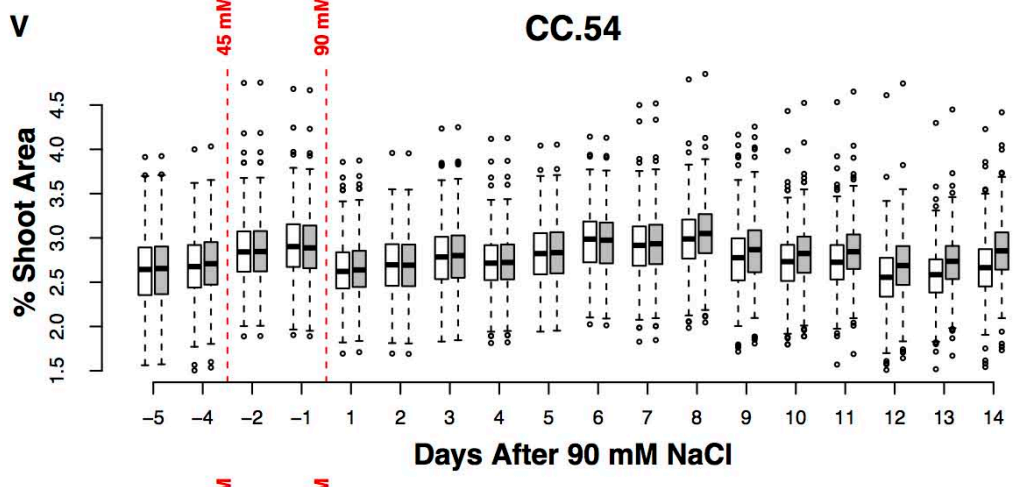
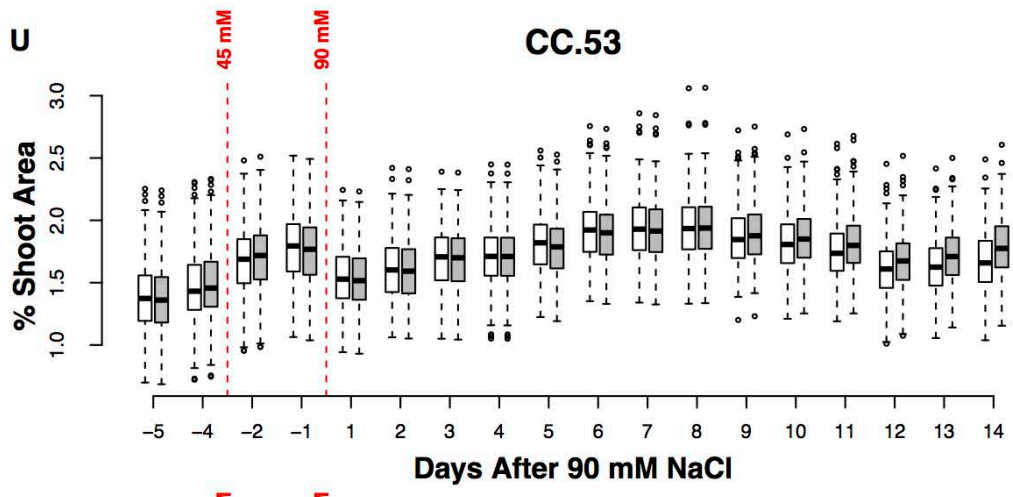


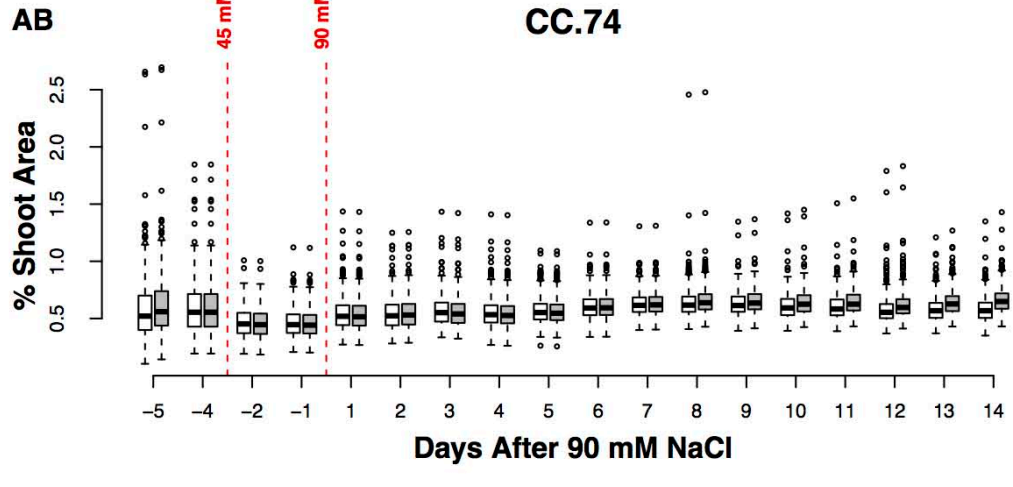
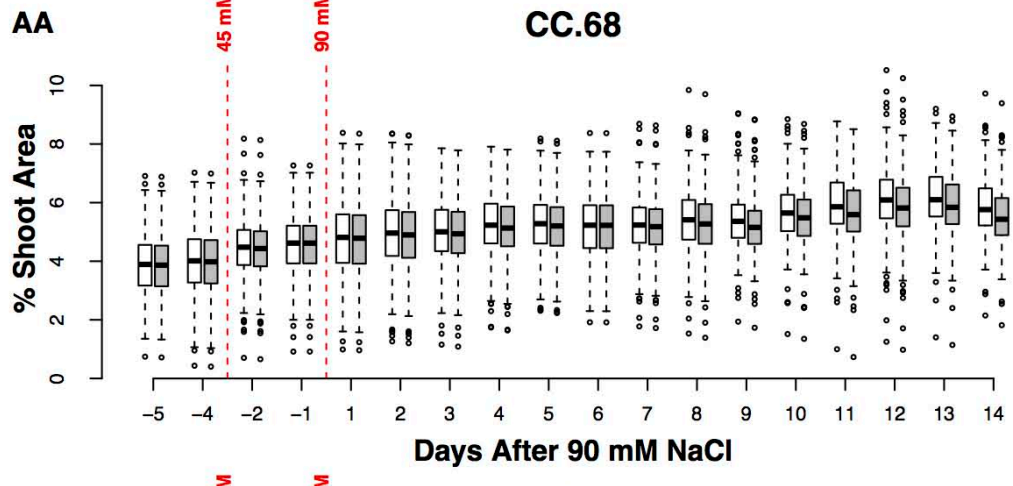
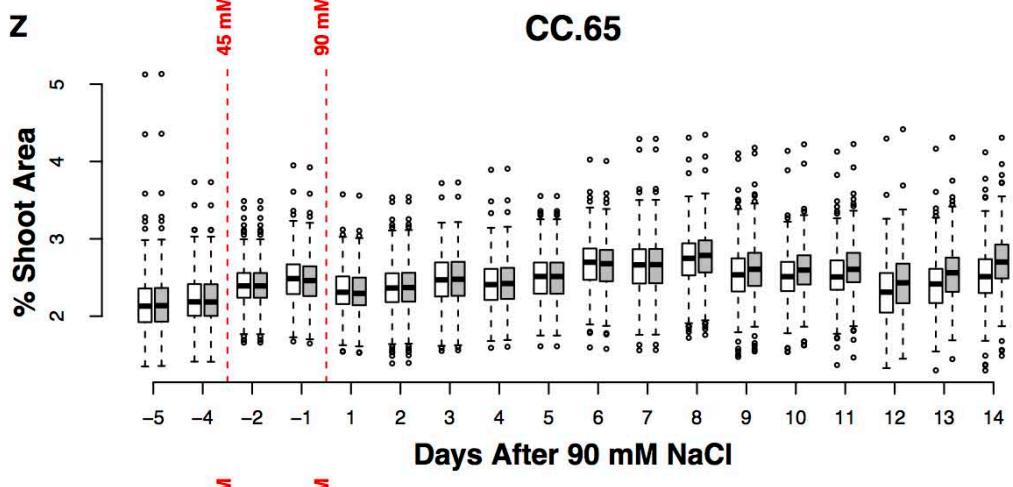
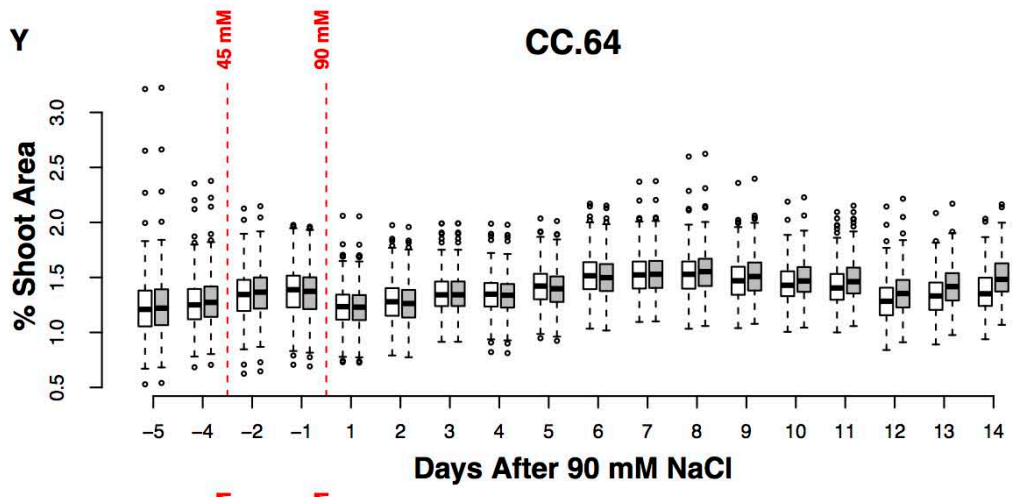












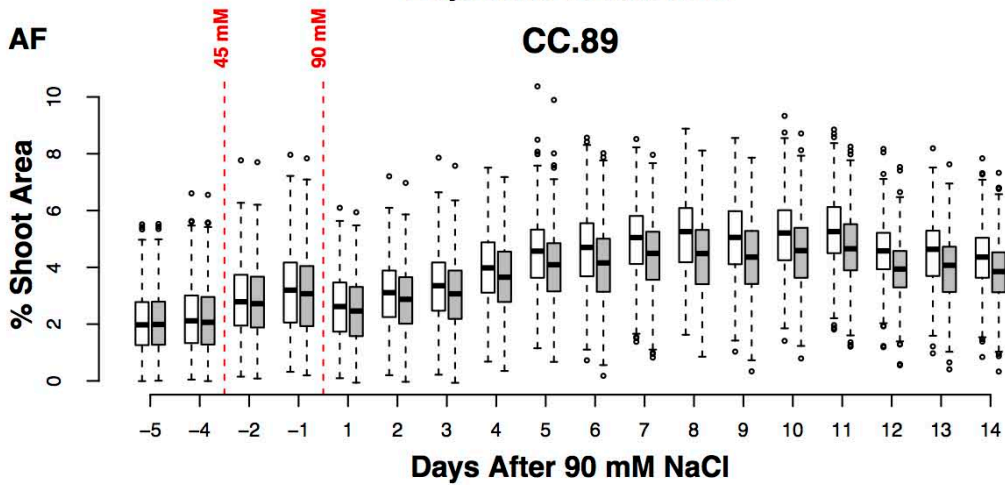
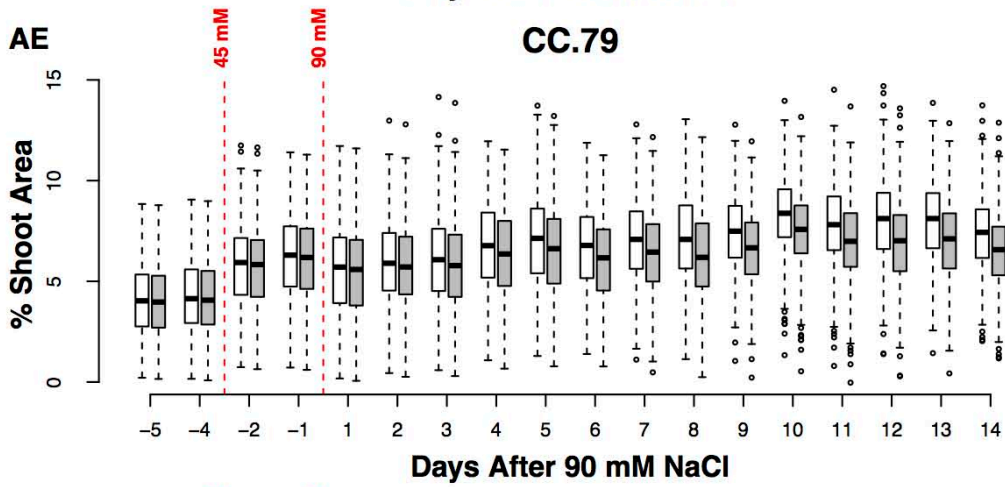
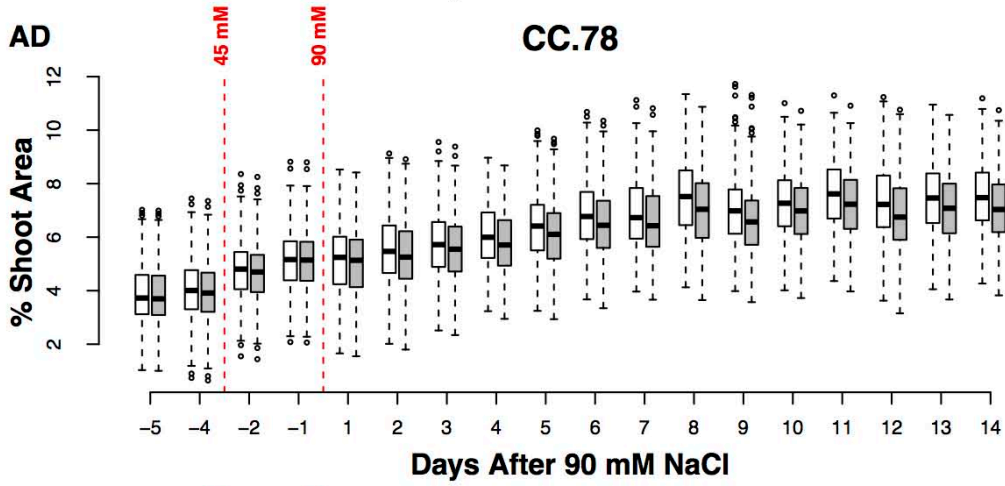
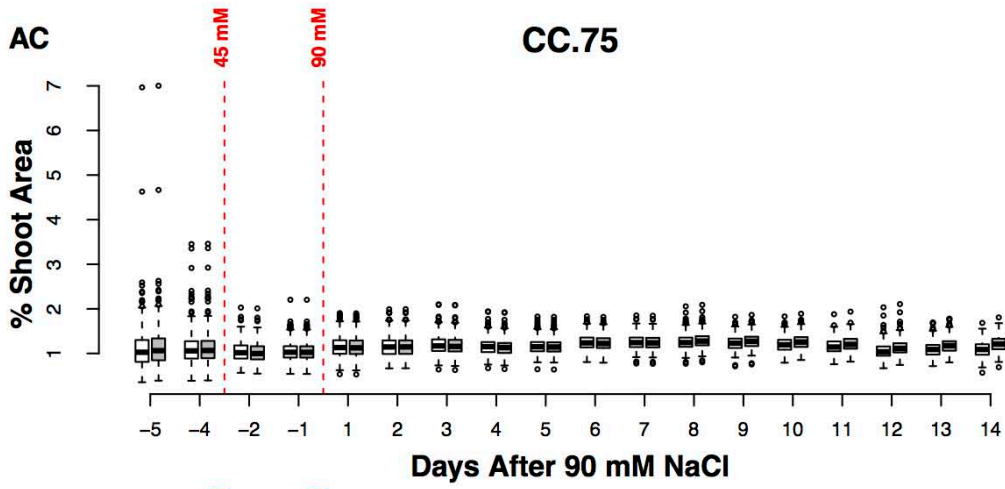
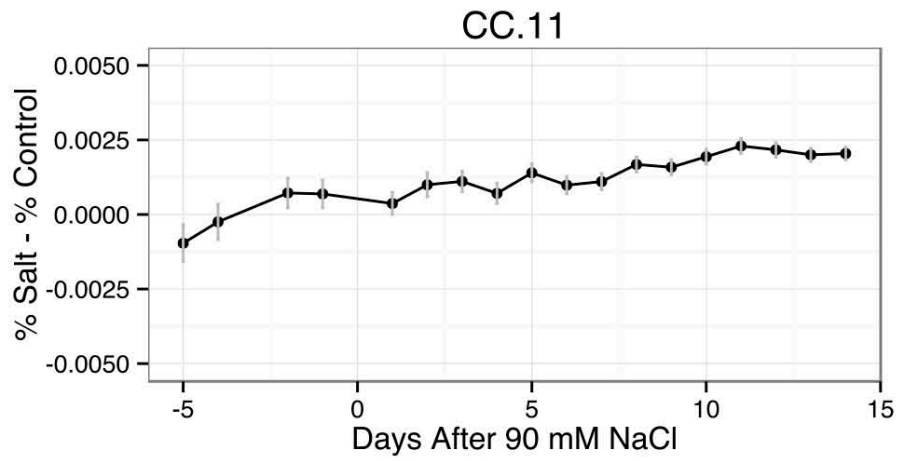
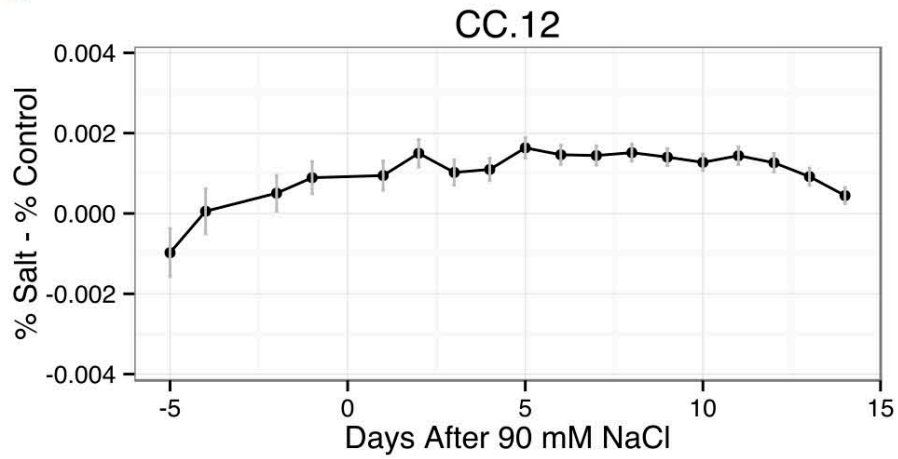
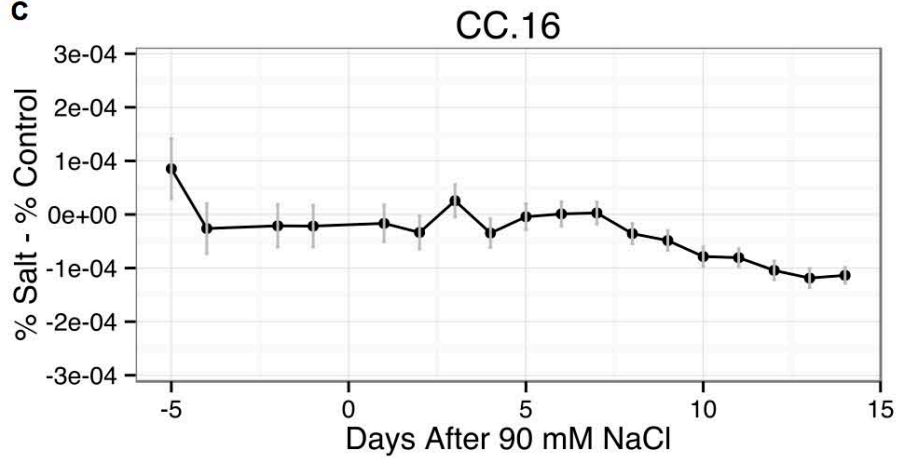
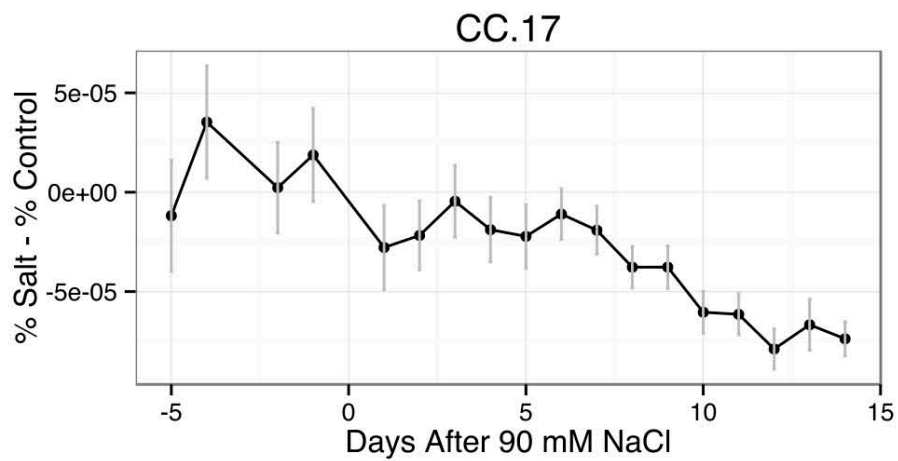
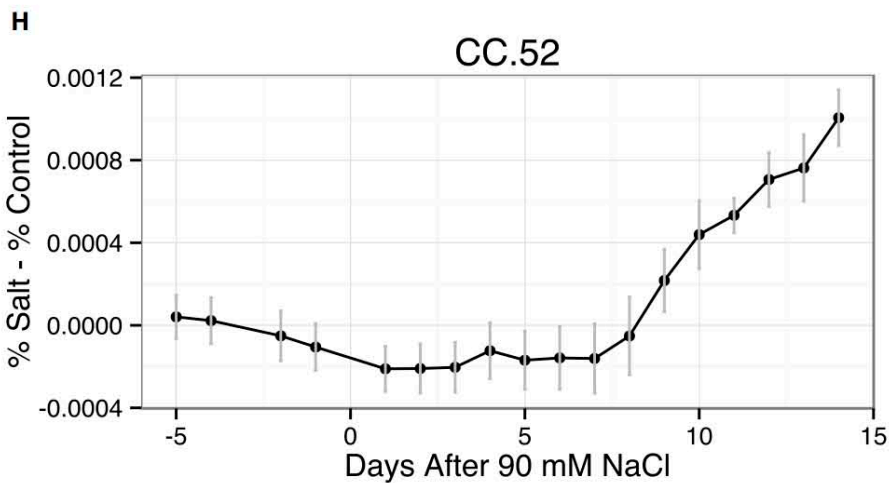
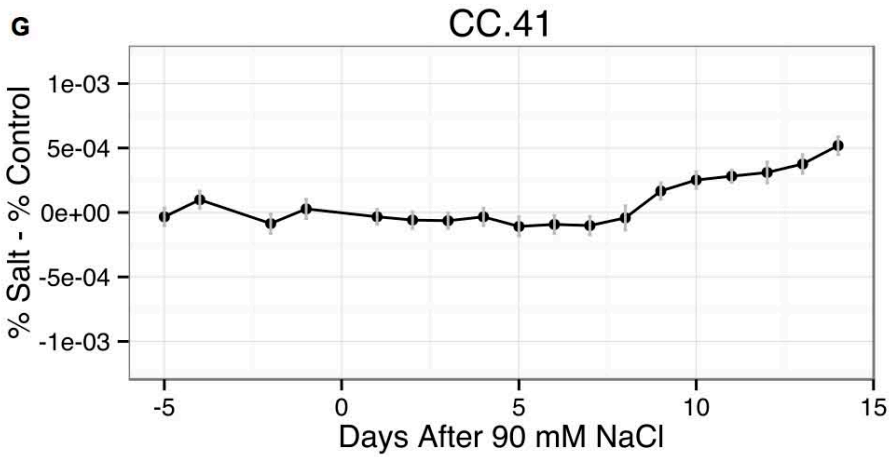
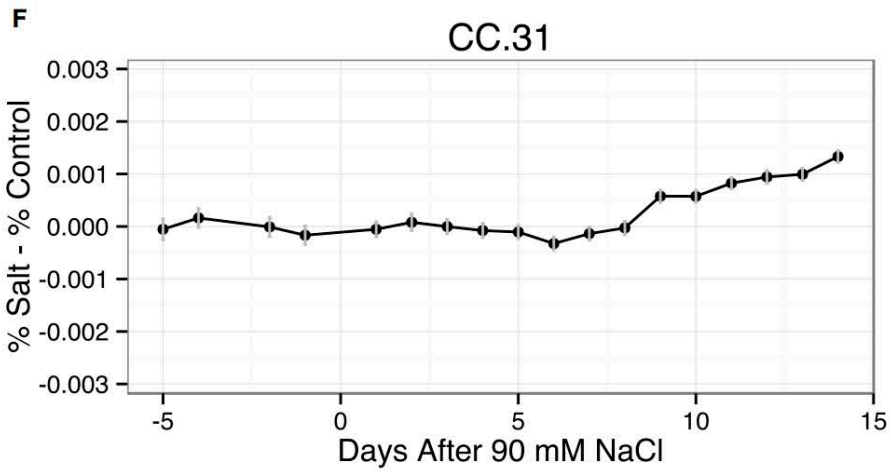
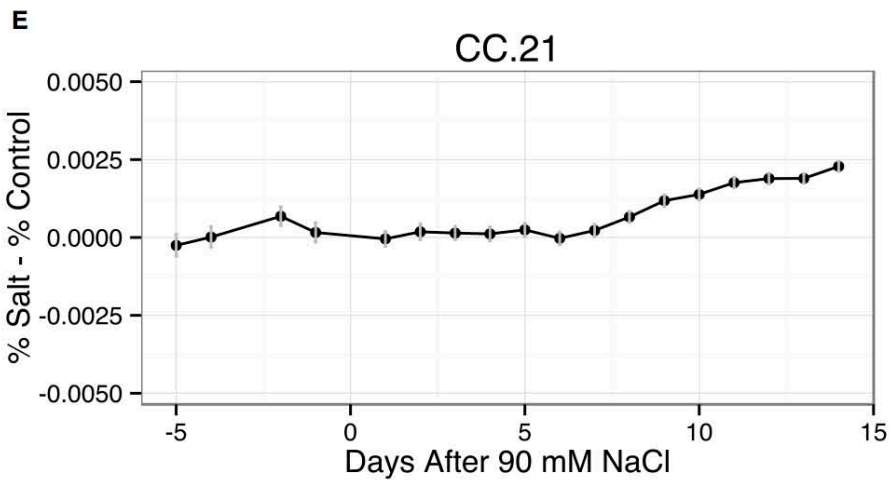
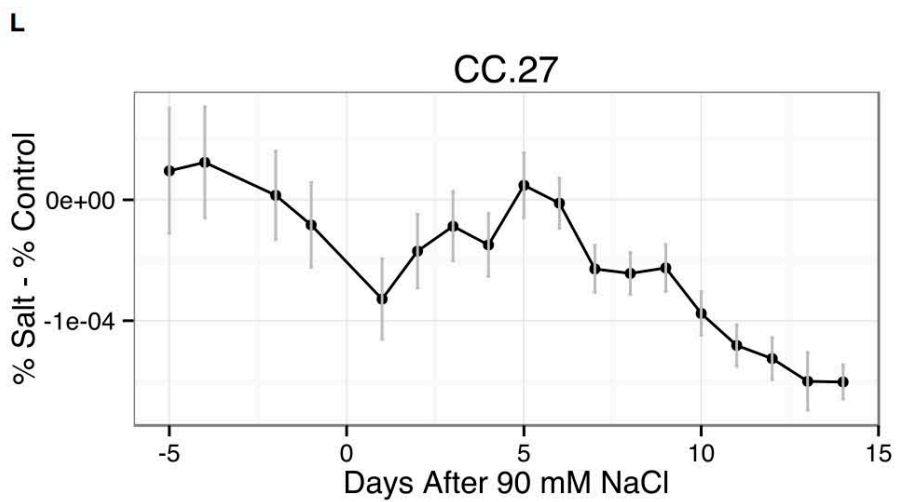
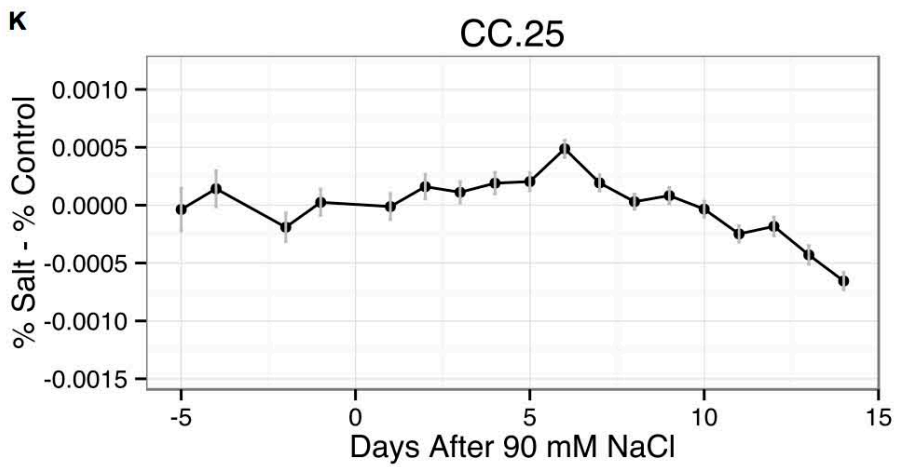
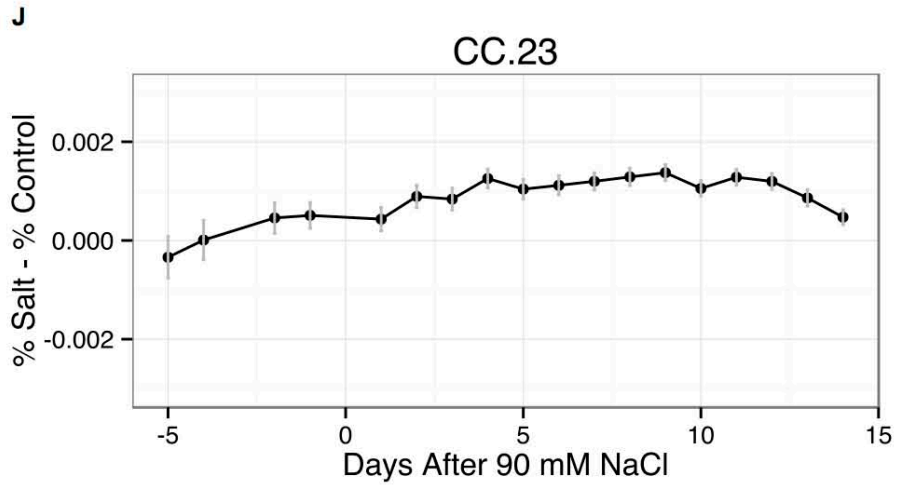
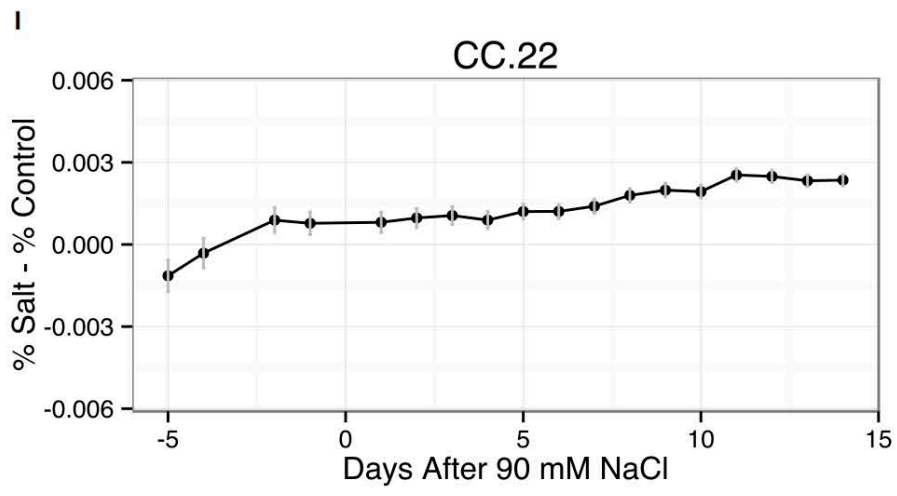


Fig S20: (A-AF) Mean temporal trends of the 32 salinity-responsive fluorescence color classes. For each color class and accession we calculated the salinity response, which is defined as the percent of total pixels from two side-view images accounted for by the color class in saline conditions minus the percent of total pixels accounted for by the class in control conditions. Error bars represent standard error.

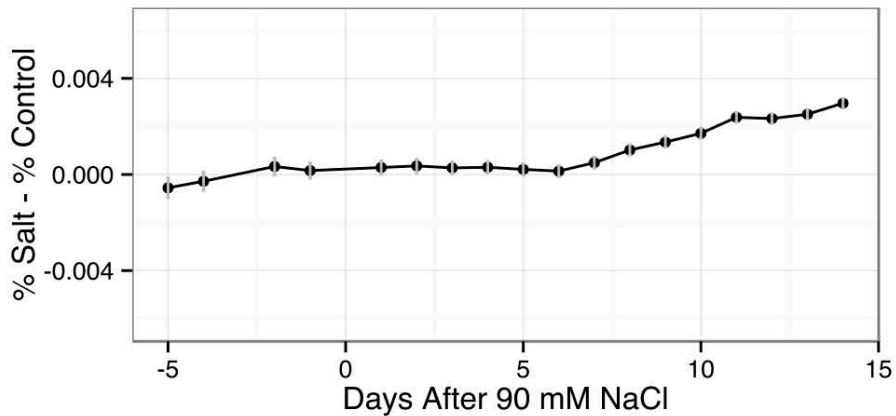
A**B****C****D**



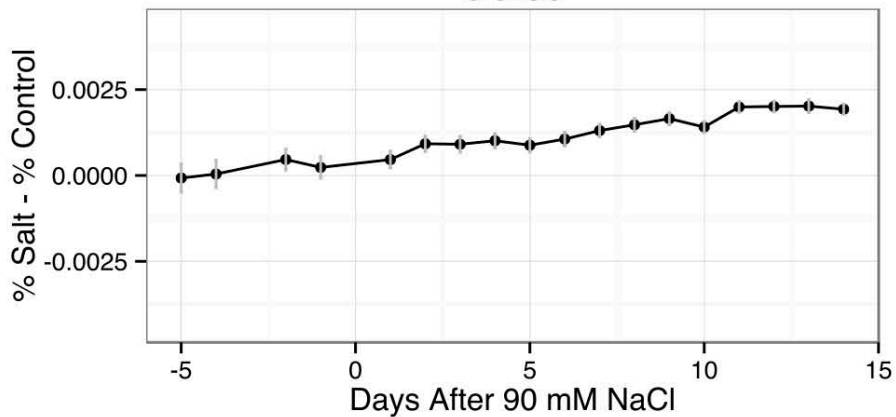


M

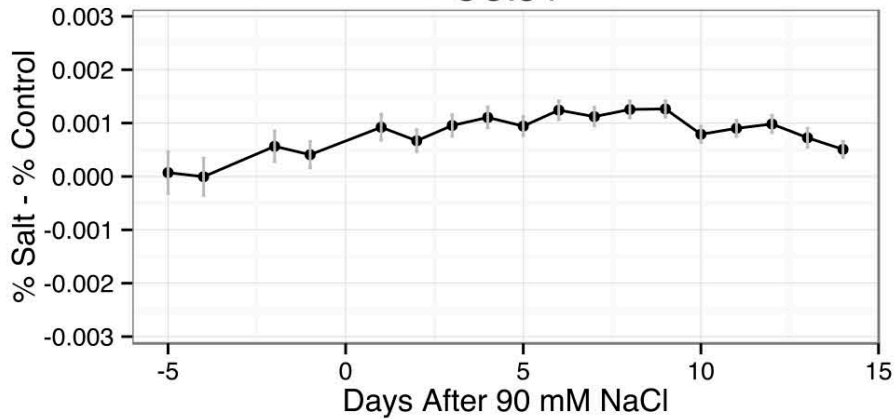
CC.32

**N**

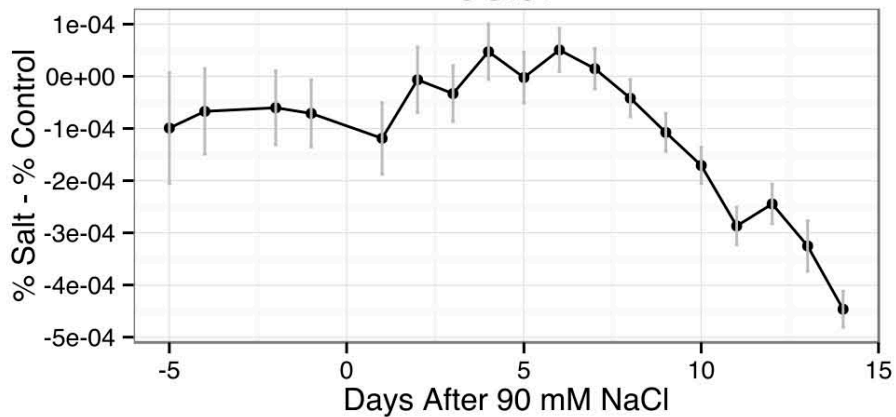
CC.33

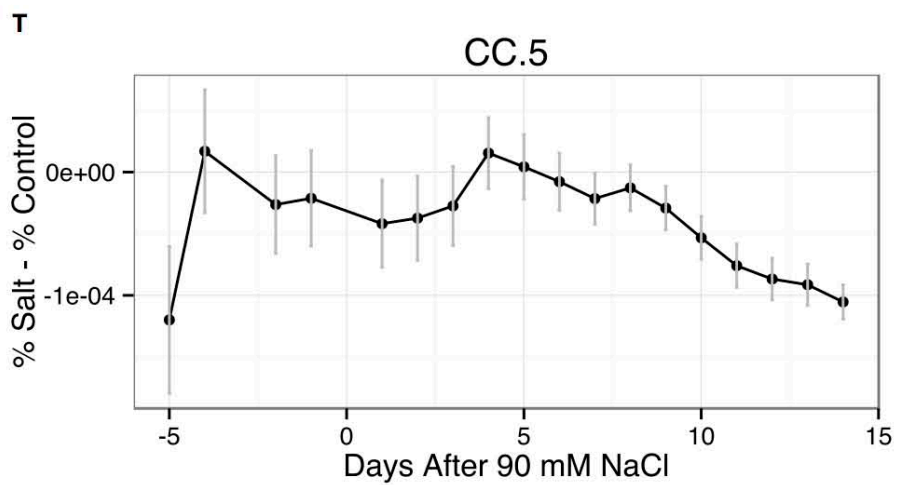
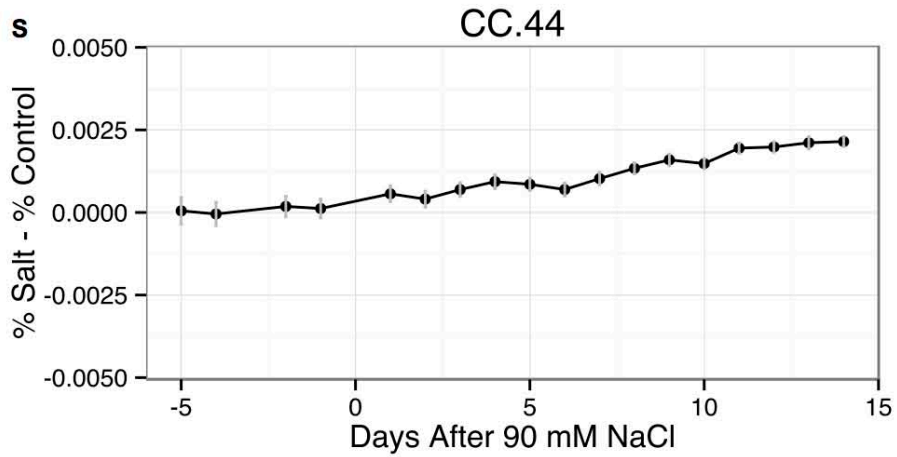
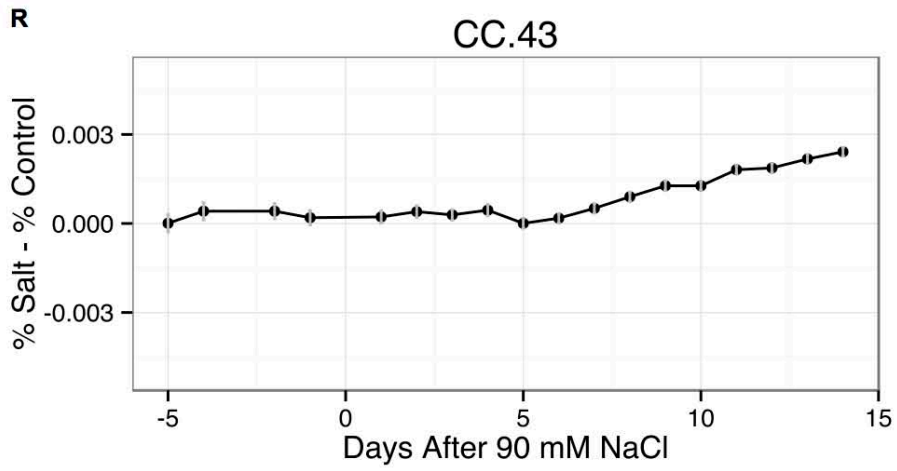
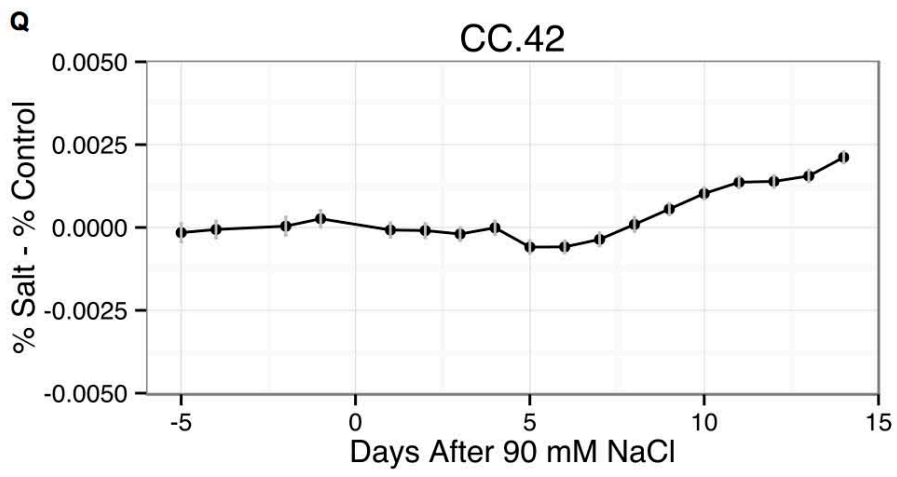
**O**

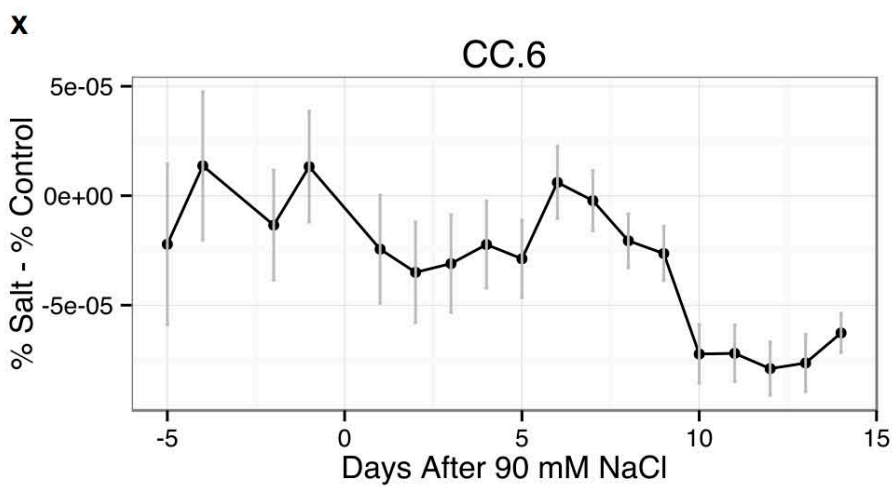
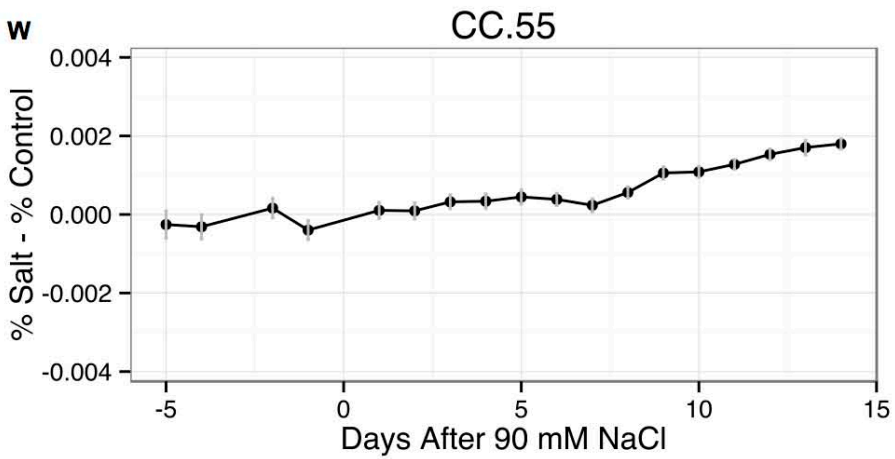
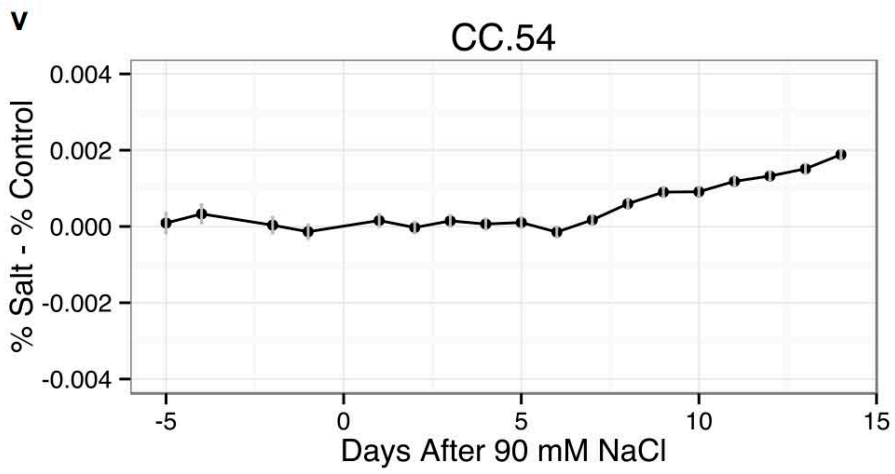
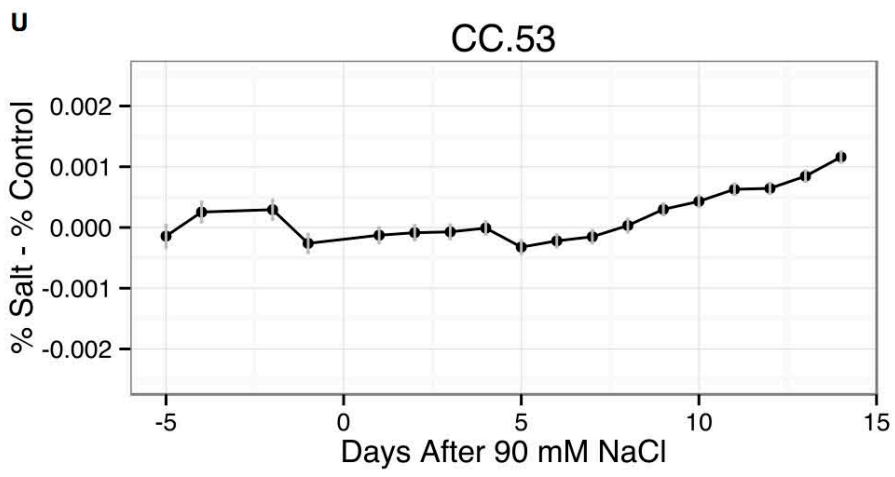
CC.34

**P**

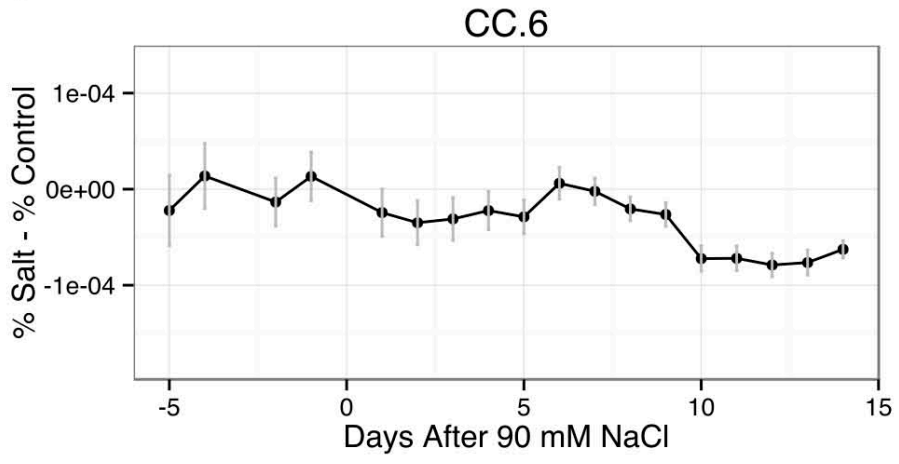
CC.37



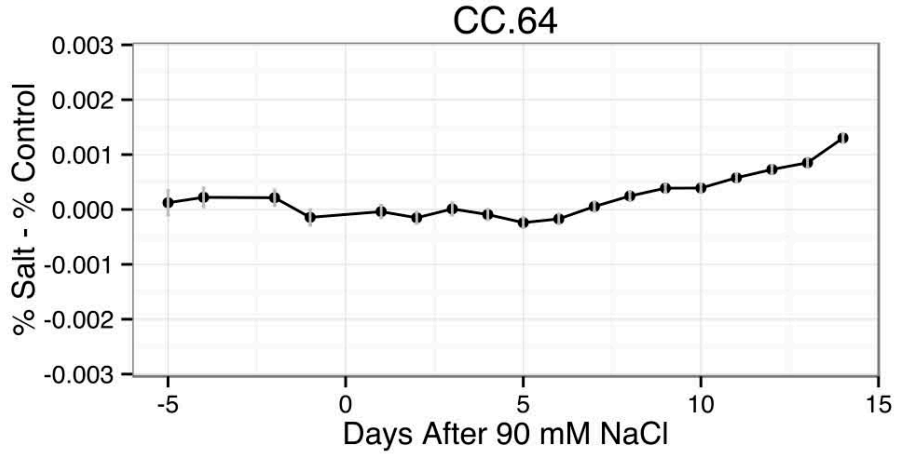




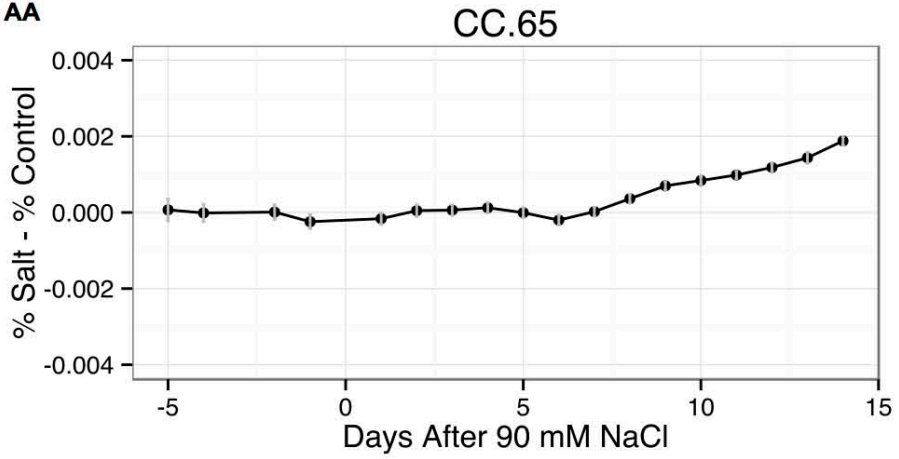
Y



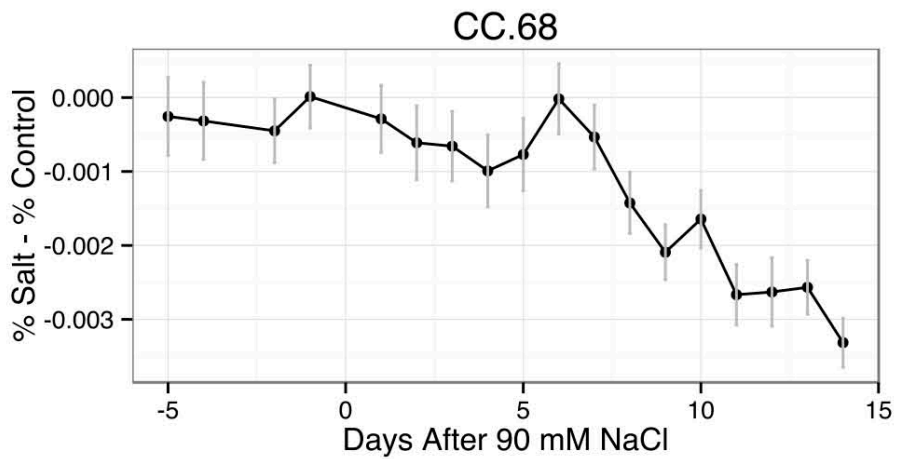
Z



AA

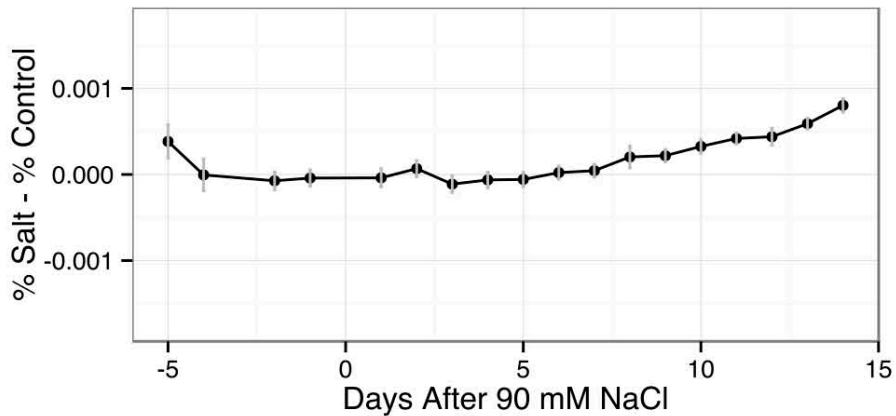


AB



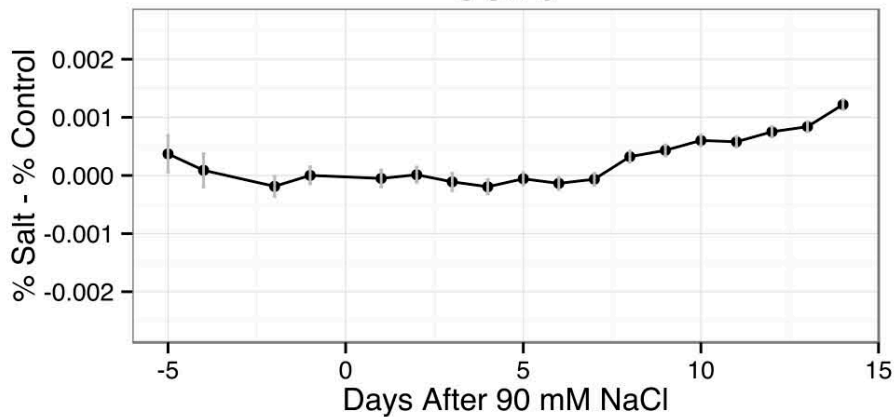
AC

CC.74



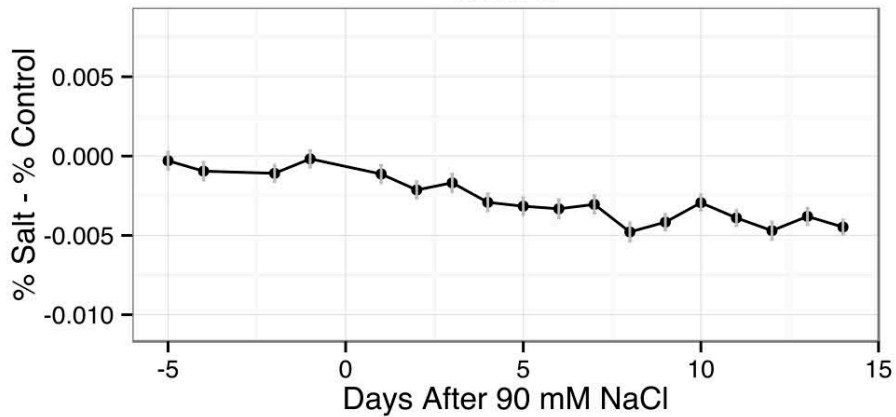
AD

CC.75



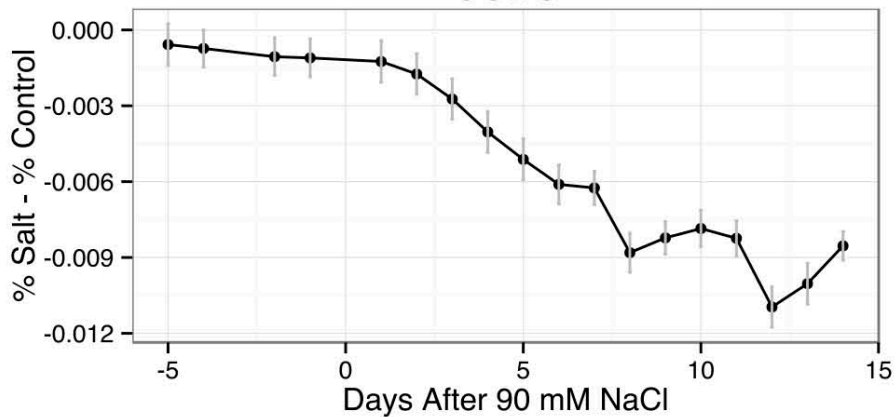
AE

CC.78



AF

CC.79



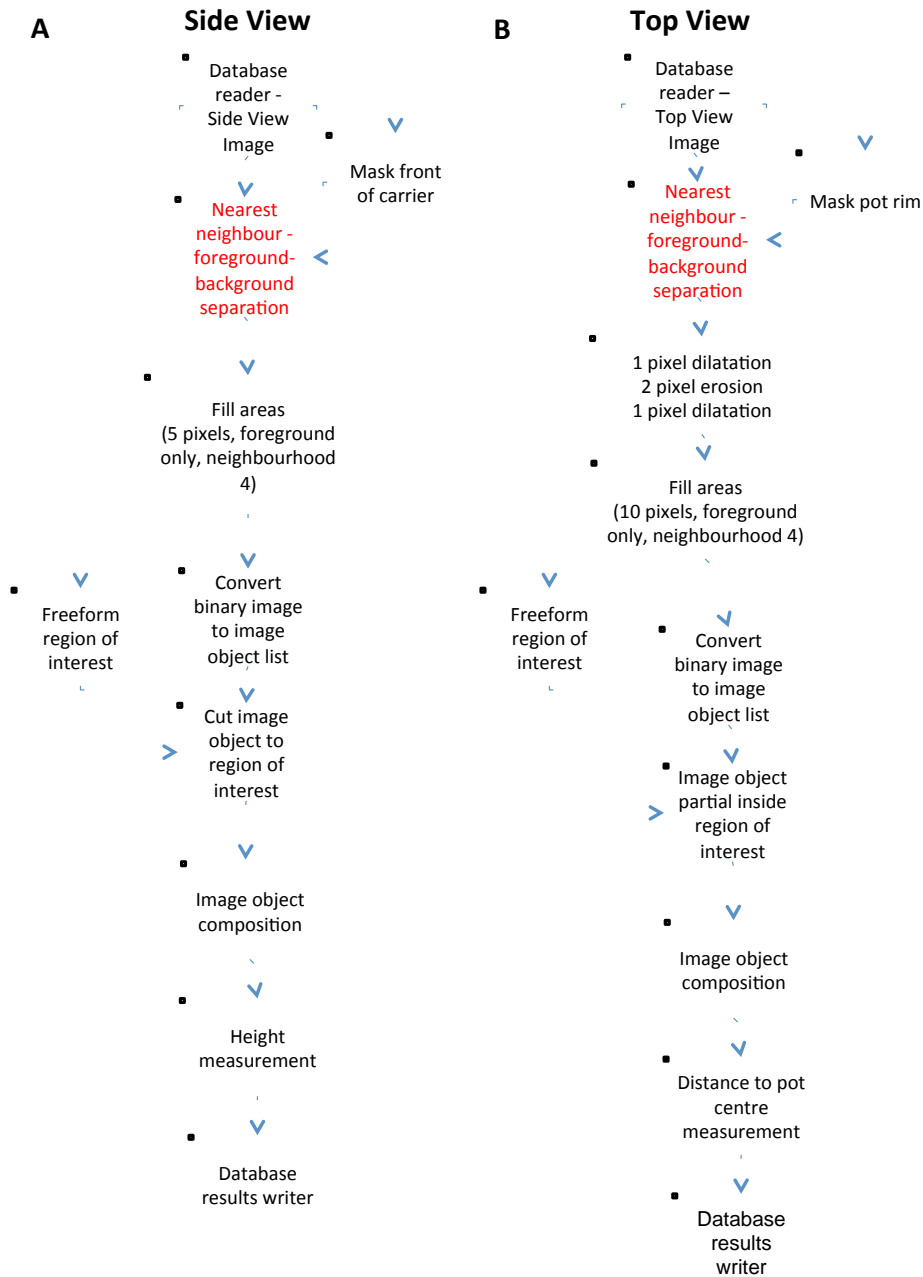


Figure S21. LemnaGrid pipeline used to process RGB side (A) and top (B) view images.

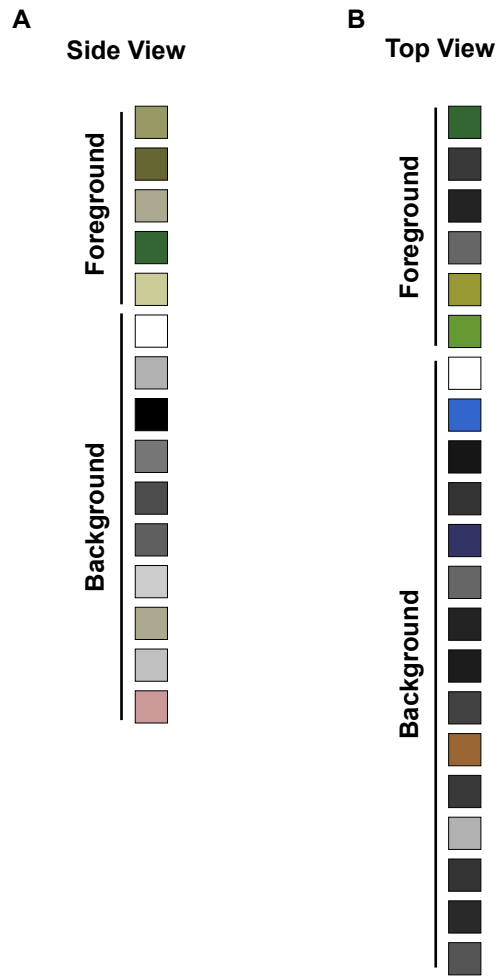


Figure S22. Color classes used to define foreground and background pixels from RGB side view (A) and top view (B) images for the LemnaGrid Nearest Neighbor foreground-background colour separation method.

S1 Table: Seven digital traits used to describe plant growth responses.

Abbreviation	Image Type	Processing Platform	View	Definition
MinR SV	RGB (Visible)	LemnaGrid	SV1 + SV2	The area of the minimum-enclosing rectangle enclosing the object.
MinC SV	RGB (Visible)	LemnaGrid	SV1 + SV2	The diameter of the minimum enclosing circle enclosing the object.
ConC SV	RGB (Visible)	LemnaGrid	SV1 + SV2	Circumference of the convex hull for the object.
ConA SV	RGB (Visible)	LemnaGrid	SV1 + SV2	Area of the convex hull for the object.
Ci SV	RGB (Visible)	LemnaGrid	SV1 + SV2	The circumference of the minimum circle that encloses the plant.
CL SV	RGB (Visible)	LemnaGrid	SV1 + SV2	The greatest distance between any of the points within the convex hull.
PSA	RGB (Visible)	LemnaGrid	SV1 + SV2 + TV	Projected Surface Area. Sum of plant pixels from each view.

The convex hull is the smallest shape that encloses a set of points X , so that any line drawn between points of X is enclosed within the shape.

Table S3. Candidate genes underlying significant SNPs. All genes within 200kb of a significant SNP were considered as possible candidates. A significance threshold of $p < 10^{-8}$ was used for logistic growth-response association analysis, and $p < 10^{-7}$ for GWA of salinity-induced fluorescence responses. SNP positions are based on MSU build 7.

Trait(s)	Chr.	SNP Position	SNP ID	p-value	Rice Gene	Rice Annotation	Arabidopsis Annotation	Reference(s)
Growth	1	7447351	dd1001171	1.89E-11	LOC_Os01g13460	Helix-loop-helix DNA-binding domain containing protein	AT2G46510	AIB (Li et al., 2007)
Growth	2	32258316	id2014363	5.79E-10	LOC_Os02g52780	bZIP transcription factor	AT3G19290	ABF4 (Choi et al., 2005)
Growth	3	11079914	id3005794	2.25E-10	LOC_Os03g19720	EF hand family protein	AT5G49480	AtCP1 (Jang et al., 1998)
Growth	3	16293444	id3008139	1.11E-16	LOC_Os03g28120	Potassium channel protein	AT2G26650	AKT1 (Hirsch et al., 1998)
Growth	6	27647390	id6015813	2.81E-09	LOC_Os06g45940	Potassium transporter	AT2G30070	AtKT1 -
Growth	7	26461039	id7005111	9.45E-09	LOC_Os07g44290	CAMK-KIN1/SNF1/Nim1-like.29	AT3G17510	CIPK1 (D'Angelo et al., 2006)
Growth	9	879018	ud9000038	7.15E-09	LOC_Os09g02214	Citrate transporter protein	AT3G19490	AtNHD1 (Müller et al., 2014)
Growth	9	16562832	id9005164	2.05E-11	LOC_Os09g27580	Potassium transporter	AT2G30070	AtKT1 -
Growth	12	25277179	id12009128	1.17E-10	LOC_Os12g40830	PFKB kinase family	AT5G37850	AtSOS4 (Shi et al., 2002)
Growth	1	25003341	id1014913	3.18E-11	LOC_Os01g43410	CAMK-like.9	AT4G23650	CDPK6 (Latz et al., 2013)
FLUO (cc.41)	1	27738377	id1016079	2.57E-08	LOC_Os01g48680	Two pore calcium channel protein 1	AT4G03560	AtCCH1 (Choi et al., 2014)
FLUO (cc.41, cc.52)	1	29950678	id1017845	4.11E-09	LOC_Os01g52070	Potassium channel	AT4G32650	AtKC1 (Geiger et al., 2009)
FLUO (cc.31, cc.41, cc.52)	1	30454089	id1018311	6.52E-08	LOC_Os01g53294	Respiratory burst oxidase protein B	AT1G64060	RBOH F (Ma et al., 2012)

Table S4. LemnaGrid devices used for processing RGB images and corresponding ImageHarvest/OpenCV functions.

LemnaGrid Device	LemnaGrid Parameters	Definition	ImageHarvest Function(s)*
Nearest Neighbor foreground-background colour separation	5 foreground colors, 10 background colors (see Fig. S21 for colors)	A set of colours are selected in that represent background and foreground objects. Each pixel in the image is assigned to background or foreground class using nearest neighbour method.	knn(self, k labels) self: class containing image k: number of foreground colors classes labels: List of BGR (blue, green, red) ranges that define the plant/foreground object
Fill Holes	Five pixels (foreground only); neighborhood 4	A hole, which is defined as a background area that is completely surrounded by the foreground object, is filled using the user-defined parameters and is added to the foreground object.	cv2.findContours(img,cv2.RETR_CCOMP,cv2.CHAIN_APPROX_SIMPLE) img: An 8-bit single-channel image cv2.RETR_CCOMP: Contour retrieval mode (see OpenCV documentation for complete description) cv2.CHAIN_APPROX_SIMPLE: Contour approximation method (see OpenCV documentation for complete description) cv2.drawContours(img,contour) img: An 8-bit single-channel image
Morphological Filter	1 pixel dilation, 2 pixel erosion, 1 pixel dilation	This device performs a defined series of pixel size reduction steps on a binary image to eliminate small noise from the foreground object.	cv.Erode(src, dst, element=None, iterations=1) cv.Dilate(src, dst, element=None, iterations=1) src: source image dst: output image of the same size as src element: a structuring element used for erosion/dilation

*LemnaGrid is a proprietary software, and while these functions may be related to LemnaGrid devices they are not exact replicates.

References

- Choi H, Park H-J, Park JH, Kim S, Im M-Y, Seo H-H, Kim Y-W, Hwang I, Kim SY** (2005) Arabidopsis calcium-dependent protein kinase AtCPK32 interacts with ABF4, a transcriptional regulator of abscisic acid-responsive gene expression, and modulates its activity. *Plant Physiol* **139**: 1750–1761
- Choi W-G, Toyota M, Kim S-H, Hilleary R, Gilroy S** (2014) Salt stress-induced Ca²⁺ waves are associated with rapid, long-distance root-to-shoot signaling in plants. *Proc Natl Acad Sci U S A* **111**: 6497–502
- D'Angelo C, Weint S, Batistic O, Pandey GK, Cheong YH, Schültke S, Albrecht V, Ehlert B, Schulz B, Harter K, et al** (2006) Alternative complex formation of the Ca²⁺-regulated protein kinase CIPK1 controls abscisic acid-dependent and independent stress responses in Arabidopsis. *Plant J* **48**: 857–872
- Geiger D, Becker D, Vosloh D, Gambale F, Palme K, Rehers M, Anschuetz U, Dreyer I, Kudla J, Hedrich R** (2009) Heteromeric AtKC1{middle dot}AKT1 channels in Arabidopsis roots facilitate growth under K⁺-limiting conditions. *J Biol Chem* **284**: 21288–95
- Hirsch RE, Lewis BD, Spalding EP, Sussman MR** (1998) A role for the AKT1 potassium channel in plant nutrition. *Science* **280**: 918–921
- Jang HJ, Pih KT, Kang SG, Lim JH, Jin JB, Piao HL, Hwang I** (1998) Molecular cloning of a novel Ca²⁺-binding protein that is induced by NaCl stress. *Plant Mol Biol* **37**: 839–847
- Latz A, Mehlmer N, Zapf S, Mueller TD, Wurzinger B, Pfister B, Csaszar E, Hedrich R, Teige M, Becker D** (2013) Salt stress triggers phosphorylation of the Arabidopsis vacuolar K⁺ channel TPK1 by calcium-dependent protein kinases (CDPKs). *Mol Plant* **6**: 1274–89
- Lenth R V, Hervé M** (2015) lsmeans: Least-Squares Means.
- Li H, Sun J, Xu Y, Jiang H, Wu X, Li C** (2007) The bHLH-type transcription factor AtAIB positively regulates ABA response in Arabidopsis. *Plant Mol Biol* **65**: 655–665

Ma L, Zhang H, Sun L, Jiao Y, Zhang G, Miao C, Hao F (2012) NADPH oxidase AtrbohD and AtrbohF function in ROS-dependent regulation of Na⁺/K⁺ homeostasis in Arabidopsis under salt stress. *J Exp Bot* **63**: 305–317

Müller M, Kunz HH, Schroeder JI, Kemp G, Young HS, Ekkehard Neuhaus H (2014) Decreased capacity for sodium export out of Arabidopsis chloroplasts impairs salt tolerance, photosynthesis and plant performance. *Plant J* **78**: 646–658

R Core Team (2014) R: A Language and Environment for Statistical Computing.

Shi H, Shi H, Xiong L, Xiong L, Stevenson B, Stevenson B, Lu T, Lu T, Zhu J, Zhu J (2002) The Arabidopsis. *Plant Cell* **14**: 575–588